J. Math. Biol. (2016) 72:123–156
DOI 10.1007/s00285-015-0883-2

Mathematical Biology

From invasion to latency: intracellular noise and cell motility as key controls of the competition between resource-limited cellular populations

Pilar Guerrero[1] · **Helen M. Byrne**[2,3] · **Philip K. Maini**[2] · **Tomás Alarcón**[4,5]

Received: 13 August 2014 / Revised: 17 February 2015 / Published online: 2 April 2015

Abstract In this paper we analyse stochastic models of the competition between two resource-limited cell populations which differ in their response to nutrient availability: the resident population exhibits a switch-like response behaviour while the invading population exhibits a bistable response. We investigate how noise in the intracellular regulatory pathways and cell motility influence the fate of the incumbent and invading populations. We focus initially on a spatially homogeneous system and study in detail the role of intracellular noise. We show that in such well-mixed systems, two distinct

Electronic supplementary material The online version of this article (doi:10.1007/s00285-015-0883-2) contains supplementary material, which is available to authorized users.

✉ Tomás Alarcón
tomasalarc@gmail.com; talarcon@crm.cat

Pilar Guerrero
pguerrero@ucl.ac.uk

Helen M. Byrne
byrne@maths.ox.ac.uk

Philip K. Maini
maini@maths.ox.ac.uk

1 Department of Mathematics, University College London, Gower Street, London WC1E 6BT, UK

2 Wolfson Centre for Mathematical Biology, Mathematical Institute, University of Oxford, Oxford OX2 6GG, UK

3 Department of Computer Science, Computational Biology Group, University of Oxford, Oxford OX1 3QD, UK

4 Centre de Recerca Matemàtica, Campus de Bellaterra, Edifici C, 08193 Bellaterra, Barcelona, Spain

5 Departament de Matemàtiques, Universitat Atonòma de Barcelona, 08193 Bellaterra, Barcelona, Spain

regimes exist: In the low (intracellular) noise limit, the invader has the ability to invade the resident population, whereas in the high noise regime competition between the two populations is found to be neutral and, in accordance with neutral evolution theory, invasion is a random event. Careful examination of the system dynamics leads us to conclude that (i) even if the invader is unable to invade, the distribution of survival times, $P_S(t)$, has a fat-tail behaviour ($P_S(t) \sim t^{-1}$) which implies that small colonies of mutants can coexist with the resident population for arbitrarily long times, and (ii) the bistable structure of the invading population increases the stability of the latent population, thus increasing their long-term likelihood of survival, by decreasing the intensity of the noise at the population level. We also examine the effects of spatial inhomogeneity. In the low noise limit we find that cell motility is positively correlated with the aggressiveness of the invader as defined by the time the invader takes to invade the resident population: the faster the invasion, the more aggressive the invader.

Keywords Invasion · Latency · Noise · Motility

Mathematics Subject Classification 92D25 · 97M60 · 60J80

1 Introduction

The aim of this paper is to analyse competition between two cell populations which employ different strategies to exploit a shared resource, i.e. they differ in how they transform the available resource into offspring. In practice, these strategies are controlled by complex signalling pathways which control gene expression and protein synthesis in response to varying resource availability (see, for example Alarcón et al. (2004), Bedessem and Stéphanou (2014), where models of how oxygen concentration regulates cell-cycle progression are proposed). Cell activity can then be described in terms of so-called "response curves". These curves represent the level of activation of a gene or the concentration of a protein driving a particular cellular response as a function of the concentration of a substance (in our case, the resource, e.g. oxygen) or the level of some stimulus. We consider the case in which the response curve represents the steady-state level of the corresponding output as a function of the stimulus Alarcón and Page (2007). Two typical response curves are shown in Fig. 1 and described below.

As stated above, we analyse the competition between two populations whose cells exhibit different response curves. We consider a resident population of cells with a switch-like response curve similar to that represented in Fig. 1(a) and we interpret this curve in the following way: when the concentration of the resource is below a threshold value (c_0, in Fig. 1(a)), proliferation cannot be activated. Such cells remain in a quiescent state and will eventually die. If the resource concentration exceeds c_0, proliferation can occur (i.e. the cell-cycle is activated) and the cell will divide.

We consider that this population of *switch-like* cells is in competition with an invading or mutant population of cells characterised by a bistable response curve (see Fig. 1(b)) whose interpretation is more involved. When the resource concentration falls below c_1 (see Fig. 1(b)), proliferation is assumed to be inactive and the corresponding

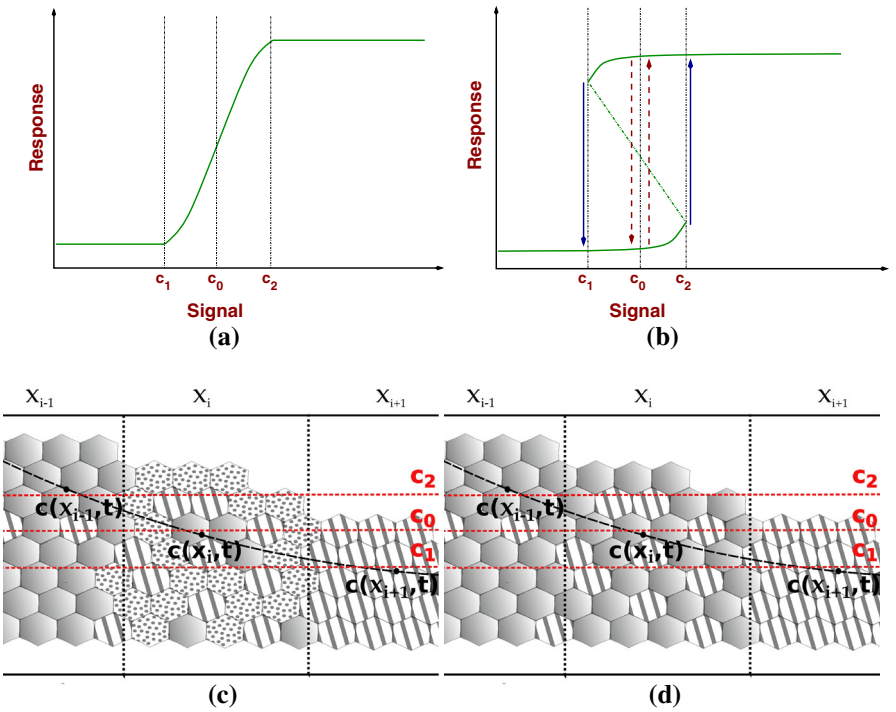

Fig. 1 Response curves corresponding to two competing populations: (a) switch-like response and (b) bistable response. Plot (a) depicts a situation where the probability of triggering a particular type of cellular response (say, proliferation) increases monotonically with the intensity of the corresponding stimulus or signal (say, abundance of a resource). Plot (b) corresponds to a system where a particular cell can be in one of two *phenotypes* (corresponding to the *upper* and *lower branches*) with sharp, abrupt transitions between them. For the bistable response as shown in plot (b), we distinguish between two distinct situations: the low intracellular noise regime where transitions between phenotypes occur only when the signal concentration falls below (exceeds) c_1 (c_2), (*solid blue arrows* in panel (b)), and the high intracellular noise level, where noise-driven transitions can also occur for signal concentrations in the interval $c_1 \leq c \leq c_2$ (dashed red arrows in panel (b)). Plots (c) and (d) show how the spatially-dependent resource profile relates to the response functions shown in plots (a) and (b), respectively, and also how resource levels give rise to (local) population limitation. Both plots (c) and (d) show a spatial array of three compartments occupied by switch-like and bistable cells, respectively. Each compartment, x_{i-1}, x_i, and x_{i+1} is depicted to have a different resource concentration. The level of resource in each compartment is such that $c(x_{i-1}) > c_2$, $c(x_i) \simeq c_0, c(x_{i+1}) > c_1$, respectively. Consider a population of switch-like cells (plot (c)). Solid hexagons represent cells whose birth rate exceeds their death rate, spotted hexagons correspond to cells whose birth and death rates are equal, and striped hexagons represent cells whose death rate exceeds their birth rate. In compartment x_{i-1} where $c(x_{i-1}) > c_2$, most cells are proliferating. Cells in x_i ($c(x_i) \simeq c_0$) are as likely to proliferate as to die. Most cells in x_{i+1} ($c(x_{i+1}) \simeq c_1$) are undergoing apoptosis (see Table 1). Bistable cells (plot (d)) exhibit two types of behaviour: proliferation (solid hexagons) and quiescence (striped hexagons). In compartment x_{i-1} the former are more abundant than the latter since $c(x_{i-1}) > c_2$. In x_{i+1}, by contrast, quiescent cells are more abundant than proliferative cells since $c(x_{i+1}) < c_1$. In compartment x_i we have a mixture of proliferating and quiescent cells, their relative proportion being determined by the noise-to-activation barrier ratio (see Table 1 and Eq. (4)) (colour figure online)

cell is in a quiescent state which will eventually lead to its death. If the resource levels exceed c_2, a threshold value in Fig. 1(b), then the cell-cycle is active and the cell divides. The feature which distinguishes these cells from the resident ones is the

existence of an intermediate region of resource concentrations, $c \in [c_1, c_2]$, for which cells can be in either phenotype: quiescent or proliferating.

Both types of response curves are known to correspond to well-characterised biological situations Tyson et al. (2003). For example, Tyson et al. (2003) have shown that a sigmoidal response curve (see Fig. 1(a)) can arise if the cellular response depends on a protein whose activity is controlled by phosphorylation and dephosphorylation reactions governed by Michaelis-Menten kinetics. This mechanism yields a very steep response. Similar behaviour can be generated by multistep processes involving a cascade of phosphorylation-dephosphorylation reactions Golbeter and Koshland (1984), as occurs, for example, in the MAP kinase cascade Kholodenko (2000).

Regarding the bistable behaviour (Fig. 1(b)), several biochemical mechanisms including mutual inhibition (see Tyson et al. (2003), Tyson and Novak (2001) and Appendix A) could give rise to such a cellular response. Alternatively, double phosphorylation of a protein can generate bistable behaviour provided additional constraints are satisfied Ortega et al. (2006). From the mathematical viewpoint, such a response curve originates from a subcritical pitchfork bifurcation Strogatz (1994) of the nonlinear system regulating cell proliferation, with resource levels serving as the control parameter.

The literature is replete with examples of biological systems in which a regulatory system switches between a graded, monostable response (i.e. our switch-like response curve) and a bistable response curve. For example, Kelemen et al. (2010) have proposed a gene regulatory circuit which can exhibit switch-like and bistable behaviour, depending on the spatial distribution of epigenetic repressors: if the repressors nucleate at two segments that flank the gene, they create two interacting repressor gradients (one upstream and the other downstream of the gene) and the corresponding response is bistable. Alternatively, if repressors localise on a single segment, then the response is monostable Kelemen et al. (2010). Similarly, analysis of mathematical models has revealed that bistable activation responses in pathways involved in apoptosis Legewie et al. (2006), cell survival Legewie et al. (2007), and cell-cycle progression Ferrel and Xiong (2001) depend upon the presence of positive feedback loops. If such positive feedbacks are rendered inactive, the corresponding response curves are monotonic (switch-like) instead of bistable. Our model is thus relevant to situations in which a mixed population of cells (i.e. one population in which the feedbacks are active and a second population in which they are inactive) compete to determine which of them has the ability to invade or persist. This scenario enables us to investigate which of these response mechanisms is robust in a given environment in terms of the outcome of our competition model.

An example of a situation to which our results may be applicable is tumour growth. Once the results regarding robustness of the different response mechanisms have been established, a natural avenue for further investigation is to ascertain which factors may lead to the emergence of malignant phenotypes which are able to thrive under a variety of conditions, including the hostile environments created by treatment with chemotherapeutic drugs Kitano (2004), Tian et al. (2011). In this paper we investigate whether the intracellular noise associated with a bistable cellular response and cell motility is a feasible candidate to play such a role.

Our aim is to understand the role of intracellular noise (i.e. randomness affecting the dynamics of the underlying regulatory pathways) and cell motility on the outcome of the competition between the two populations, switch-like and bistable. In particular, the question we address here is which of these strategies has the evolutionary advantage of being able to withstand invasion by the other cell type. For the resident, switch-like population noise blurs the threshold c_0 (see Fig. 1(a)): cells with resource concentration below c_0 have a small, but finite, probability of dividing; conversely cells experiencing resource concentration above c_0 have a small, but finite, probability of becoming quiescent. The effect of noise on bistable cells is more complex. As mentioned above, the bistable response curve Fig. 1(b) can be understood as the result of a bifurcation of the underlying cell-cycle control system which means that two attractors coexist for a range of values of the resource concentration, in our case $c \in [c_1, c_2]$. If the level of (intrinsic) noise present in the proliferation pathway is low, then the phenotype of a particular bistable cell for resource level c, such that $c \in [c_1, c_2]$, is determined by the basins of attraction of each of the attractors represented by the upper and lower branches. Transitions between states are only possible if c falls below the lower threshold, c_1, or exceeds the upper threshold, c_2 Strogatz (1994). As the intracellular noise increases in intensity, stochastic transitions between both basins of attraction can occur Gardiner (2009), Maier and Stein (1996) and there is a finite probability that for $c \in [c_1, c_2]$ there are noise-induced phenotype changes in the bistable cells.

In this paper, we investigate how noise in the intracellular regulatory pathways and cell motility determine the fate of the competition between a switch-like incumbent and a bistable invader. We show that two distinct regimes exist, namely, the low (intracellular) noise limit, in which the invader has the ability to invade the resident population, and the high noise regime, in which the competition between the two populations is found to be neutral and, in accordance with neutral evolution theory, invasion is a random event with probability equal to the proportion of invasive cells initially present in the environment Kimura (1968), Demetrius et al. (2009). Further examination of the dynamics in the high-noise limit leads us to conclude that, even if the invader is unable to invade, the distribution of survival times, $P_S(t)$, has a fat-tail behaviour: $P_S(t) \sim t^{-1}$, which implies that small colonies of mutants can coexist with the resident population for arbitrarily long times. Furthermore, the bistable structure of the invading population increases the stability of the latent populations and their long-term likelihood of survival, by decreasing the noise intensity at the population level. This behaviour suggests that our system exhibits a transition to latency or dormancy when the intracellular noise of the bistable mutants increases. In the context of this work, latency refers to the state in which an invader, which is unable to colonise the resident population, persists as a small, residual population incapable of growing but not completely eliminated Alarcón and Jensen (2010). Biologically relevant examples of such latent states include tumour dormancy Willis et al. (2010) and latent infection of HIV-1-infected patients undergoing potent anti-retroviral therapy Rong and Perelson (2009). Moreover, we analyse the effects of spatial inhomogeneity and find that cell motility is positively correlated with the aggressiveness of the invader, aggressiveness being assumed to correlate with the time the invader cells take to invade the resident population. The faster the invasion, the more aggressive the invader. Thus, our model can be useful for studying the emergence of latency and also the role of cell motility in invasion.

The remainder of this paper is organised as follows. In Sect. 2 we introduce the model formulation and the numerical methodology that is used throughout the paper. In Sect. 3, we give a detailed description of the particular problem we are studying. Sections 4 and 5 contain extended discussions of our results for well-mixed and spatially-inhomogeneous systems, respectively. Finally, Section 6 is devoted to a discussion of our results as well as future work.

2 Model formulation and methodology

In this section, we introduce our general approach, model formulation and numerical methodology. We start by describing a general model of competition between cell populations that rely upon a common resource for survival. Our model is formulated in terms of a master equation for the dynamics of the cell populations coupled to a differential equation that describes the dynamics of the resource. The model is formulated in general terms, including its application to a spatially-extended system. We then specialise the model to describe competition between a resident population of switch-like cells and an invasive population of bistable cells. The section concludes with a description of our numerical methodology, namely, a *hybrid* Gillespie algorithm.

2.1 Model formulation

In order to account for spatial structure, we consider a compartmental model, where cells in each compartment are assumed to concentrate on the regularly-spaced vertices, $x_i \in \mathbb{R}^d$, of a d-dimensional lattice, $\mathcal{L}^d$, embedded in $\mathbb{R}^d$. In each compartment, we consider N_T types of competing cells. We introduce the vector $\chi^{(k)}(t) \equiv (\chi^{(k)}(x_1, t), \ldots \chi^{(k)}(x_N, t)) \equiv (\chi_1^{(k)}(t), \ldots \chi_N^{(k)}(t))$, $k = 1, \ldots, N_T$, whose components correspond to the number of cells of type k at site $x_i \in \mathbb{R}^d$ and time t.

Our model comprises a simple birth-and-death process with random migration between nearest neighbours, and a variable resource (for example, oxygen) whose concentration controls the rates of cell birth and death. We assume that the spatial distribution, $c(x, t)$, of this resource evolves as a result of diffusion and consumption by the cell populations. In more detail, we assume that the spatio-temporal evolution of the resource (for example, oxygen) is determined by the following reaction-diffusion equation:

$$\frac{\partial c}{\partial t} = D\nabla^2 c - \bar{k}c \sum_{k=1}^{N_T} \sum_{x_i \in \mathcal{L}^d} \chi^{(k)}(t)\delta(x - x_i) \tag{1}$$

where D is the corresponding diffusivity and $\bar{k}$ is the per-cell resource depletion rate. The resource is assumed to enter the system through the boundaries of the domain. In particular, in one dimension we have:

$$D \left.\frac{\partial c}{\partial x}\right|_{x=0} = h_0, \; D \left.\frac{\partial c}{\partial x}\right|_{x=L} = -h_L \tag{2}$$

where h_0 and h_L are the nutrient fluxes at the ends of the domain. We fix $h_0 - h_L = \Omega L \bar{k} c_0$, where L is the length of our one-dimensional domain where c_0 is a typical oxygen concentration, chosen to ensure that sufficient oxygen is supplied to maintain a total population (resident plus mutant) of $O(\Omega)$ per unit length. Thus, Ω measures the average per-site population that our resource can sustain. A schematic is presented in Figs. 1(c) and (d) showing how the spatially-dependent resource profile relates to the response function.

The model we propose is a stochastic, spatially extended, birth-death process with random motility between nearest neighbours, which can be described by a master equation for the probability distribution $P(\chi^{(k)}, t)$, i.e. the probability that the population be $\chi^{(k)}$ at time t. The master equation is formulated in terms of transition rates, which describe the probability that each of the different (random) events associated with the population dynamics occurs per unit of time. We assume that the birth and death rates, $\bar{b}(c)$ and $\bar{\mu}(c)$, respectively, depend on the local oxygen concentration. At each site of $\mathcal{L}^d$, cells of each type die, change phenotype or migrate at the following rates:

- *Proliferate* ($\chi_i^{(k)} \to \chi_i^{(k)} + 1$), with rate $T_{\chi_i^{(k)}+1|\chi_i^{(k)}} = \bar{b}_k(c)\chi_i^{(k)}$, where $\bar{b}_k(c)$ is the oxygen-dependent birth rate for cells of type k;
- *Die* ($\chi_i^{(k)} \to \chi_i^{(k)} - 1$), with rate $T_{\chi_i^{(k)}-1|\chi_i^{(k)}} = \bar{\mu}_k(c)\chi_i^{(k)}$, where $\bar{\mu}_k(c)$ is the oxygen-dependent death rate for cells of type k;
- *Switch phenotype from type k to type l* ($\chi_i^{(k)}, \chi_i^{(l)} \to \chi_i^{(k)} - 1, \chi_i^{(l)} + 1$), with rate $T_{\chi_i^{(k)}-1\chi_i^{(l)}+1|\chi_i^{(k)}\chi_i^{(l)}} = \bar{w}_0 e^{-H_{kl}(c)}\chi_i^{(k)}$, where w_0 is the inverse of the characteristic time scale for phenotypic switching and $P_{kl}(c) = e^{-H_{kl}(c)}$ is the oxygen-dependent probability of a switch from phenotype k to type phenotype l. (More details about $P_{kl}(c)$ are in Sect. 3);
- *Diffuse to neighbouring compartments* ($\chi_i^{(k)}, \chi_j^{(k)} \to \chi_i^{(k)} - 1, \chi_j^{(k)} + 1$), with rate $T_{\chi_i^{(k)}-1\chi_j^{(k)}+1|\chi_i^{(k)}\chi_j^{(k)}} = \frac{\bar{\nu}_k}{h^2}\chi_i^{(k)}$, where $j \in \langle i \rangle$, $\bar{\nu}_k \geq 0$ is the diffusion coefficient for cells of type k, and h is the lattice spacing. Regarding cell motility, we ignore excluded volume interactions Bruna and Chapman (2012), i.e. competition for space, assuming instead that the carrying capacity of each compartment is solely determined by resource availability.

Having defined the various transition rates, it is straightforward to state the master equation for this spatially-extended, resource-dependent birth-and-death process Lugo and McKane (2008):

$$\begin{aligned}
&\frac{\partial}{\partial t} P(\chi^{(1)}, \ldots, \chi^{(N_T)}, t) \\
&= \sum_{k=1}^{N_T} \sum_{x_i \in \mathcal{L}^d} \left[\left(\mathcal{E}^-_{\chi_i^{(k)}} - 1 \right) T_{\chi_i^{(k)}+1|\chi_i^{(k)}} P(\chi^{(1)}, \ldots, \chi^{(N_T)}, t) \right. \\
&\quad \left. + \left(\mathcal{E}^+_{\chi_i^{(k)}} - 1 \right) T_{\chi_i^{(k)}-1|\chi_i^{(k)}} P(\chi^{(1)}, \ldots, \chi^{(N_T)}, t) \right]
\end{aligned}$$

$$
\begin{aligned}
&+\sum_{k=1}^{N_T}\sum_{j\neq k}\sum_{x_i\in\mathcal{L}^d}\Bigg[\left(\mathcal{E}^-_{\chi_i^{(k)}}\mathcal{E}^+_{\chi_i^{(j)}}-1\right)T_{\chi_i^{(k)}+1\chi_i^{(j)}-1|\chi_i^{(k)}\chi_i^{(j)}}P(\chi^{(1)},\ldots,\chi^{(N_T)},t)\\
&+\left(\mathcal{E}^+_{\chi_i^{(k)}}\mathcal{E}^-_{\chi_i^{(j)}}-1\right)T_{\chi_i^{(k)}-1\chi_i^{(j)}+1|\chi_i^{(k)}\chi_i^{(j)}}P(\chi^{(1)},\ldots,\chi^{(N_T)},t)\Bigg]\\
&+\sum_{k=1}^{N_T}\sum_{x_i\in\mathcal{L}^d}\sum_{x_j\in\langle x_i\rangle}\Bigg[\left(\mathcal{E}^-_{\chi_i^{(k)}}\mathcal{E}^+_{\chi_j^{(k)}}-1\right)T_{\chi_i^{(k)}+1\chi_j^{(k)}-1|\chi_i^{(k)}\chi_j^{(k)}}P(\chi^{(1)},\ldots,\chi^{(N_T)},t)\\
&+\left(\mathcal{E}^+_{\chi_i^{(k)}}\mathcal{E}^-_{\chi_j^{(k)}}-1\right)T_{\chi_i^{(k)}-1\chi_j^{(k)}+1|\chi_i^{(k)}\chi_j^{(k)}}P(\chi^{(1)},\ldots,\chi^{(N_T)},t)\Bigg] \qquad (3)
\end{aligned}
$$

where $\mathcal{E}^{\pm}_{\chi_i^{(k)}} f(\chi_i^{(k)}) = f(\chi_i^{(k)} \pm 1)$.

2.2 Numerical methodology

We use a straightforward generalisation of the stochastic simulation algorithm (SSA) proposed by Gillespie (1976, 1977) to produce numerical results. The SSA enables us to generate sample paths or realisations of the Master Equation (3) and involves two basic steps: (i) generate the waiting time between two random events, τ_w, and (ii) determine which of the elementary events (i.e. birth, death, migration, phenotype switch) occurs and update the populations accordingly. Since our Master Equation is coupled to a reaction-diffusion equation (see Eq. (1)), we must account for this coupling in our numerical method. By definition, during the waiting time between two events, i.e. during the time interval $[t, t+\tau_w)$, the cell populations remain constant. We thus solve Eq. (1) in the interval $[t, t+\tau_w)$ with constant $\chi^{(k)} = \chi^{(k)}(t)$. In summary, our version of the SSA involves three steps:

1. Generate the waiting time between two random events, τ_w;
2. Solve Eq. (1) in the interval $[t, t+\tau_w)$ with constant $\chi^{(k)} = \chi^{(k)}(t)$;
3. Choose which elementary event occurs and update the populations accordingly.

These three steps are repeated until a stopping condition is satisfied. Step 2 involves solving an ordinary diffirential equation (ODE) or a partial differential equation (PDE), depending on whether we are considering a well-mixed system or a spatially-inhomogeneous situation, respectively. The corresponding solvers and boundary and/or initial conditions are specified in detail in Sects. 4 and 5.

3 Competition between populations with switch-like and bistable responses

The model we study in this section considers a resident population of cells endowed with a switch-like response curve (see Fig. 1(a)) and an invading population of cells exhibiting a bistable response curve (see Fig. 1(b)). For high resource concentrations the invading cells have a proliferative phenotype and divide with probability one whilst, for low resource levels, they exhibit a quiescent phenotype and undergo apoptosis

Table 1 Transition rates for our stochastic model of competition between switch-like and bistable populations

Transition rate	Event
$T_{\chi_i^{(1)}+1\|\chi_i^{(1)}} = \tau_p^{-1} \frac{e^{\bar{\alpha}_0(c-c_0)}}{e^{\bar{\alpha}_0(c-c_0)}+e^{-\bar{\alpha}_0(c-c_0)}} \chi_i^{(1)}$	Division of switch-like cell
$T_{\chi_i^{(1)}-1\|\chi_i^{(1)}} = \tau_p^{-1} \frac{e^{-\bar{\alpha}_0(c-c_0)}}{e^{\bar{\alpha}_0(c-c_0)}+e^{-\bar{\alpha}_0(c-c_0)}} \chi_i^{(1)}$	Switch-like cell death
$T_{\chi_i^{(2)}+1\|\chi_i^{(2)}} = \tau_p^{-1} \chi_i^{(2)}$	Proliferation of bistable cell
$T_{\chi_i^{(3)}+1,\chi_i^{(2)}-1\|\chi_i^{(3)},\chi_i^{(2)}} = \bar{w}_0 e^{-H_{PA}(c)} \chi_i^{(2)}$	Bistable cell phenotype change (proliferating to quiescent)
$T_{\chi_i^{(2)}+1,\chi_i^{(3)}-1\|\chi_i^{(2)},\chi_i^{(3)}} = \bar{w}_0 e^{-H_{AP}(c)} \chi_i^{(3)}$	Bistable cell phenotype change (quiescent to proliferating)
$T_{\chi_i^{(3)}-1\|\chi_i^{(3)}} = \tau_p^{-1} \chi_i^{(3)}$	Quiescent cell death
$T_{\chi_i^{(k)}-1\chi_j^{(k)}+1\|\chi_i^{(k)}\chi_j^{(k)}} = \frac{\bar{v}_k}{h^2} \chi_i^{(k)}$	Cell migration $\forall k$ and $\forall j \in < i >$

with probability one. However, there is a regime of intermediate values of resource concentration for which transitions between the two phenotypes occur with finite probability (see Fig. A1, Supplementary Material). The question we address here is which of these strategies (i.e. switch-like or bistable response), has the evolutionary advantage of being able to withstand invasion by the other cell type.

Our model is defined by the following quantities and parameters. There are three distinct cell types ($N_T = 3$) corresponding to resident (switch-like) cells, $\chi^{(1)}$, proliferating mutant (bistable) cells, $\chi^{(2)}$, and quiescent mutant (bistable) cells $\chi^{(3)}$. The evolution of the resource concentration is given by Eq. (1). The dynamics of the cell populations is determined by the transition rates of the Master Equation (Eq. (3)) stated in Table 1.

We further assume that random changes of phenotype in the bistable population are the result of an activated process which can be modelled by rates of Arrhenius type, i.e. $P_{AP}(c) = e^{-H_{AP}(c)}$ and $P_{PA}(c) = e^{-H_{PA}(c)}$, where $P_{AP}(c)$ and $P_{PA}(c)$ are the probabilities of switching between the quiescent and proliferative phenotypes. The motivation for this modelling assumption is discussed in detail in Appendix A. The functions $H_{AP}(c)$ and $H_{PA}(c)$ depend on the height of the activation barrier relative to the noise intensity and the concentration of resources Gardiner (1983, 2009), Hanggi et al. (1990) in the following way:

$$H_{PA}(c) = \begin{cases} \bar{\delta_2}(c-c_2)^n + \bar{\alpha}_2(c_2-c_1) & \text{for } c > c_2 \\ \bar{\alpha}_2(c-c_1) & \text{for } c_1 < c \leq c_2 \\ 0 & \text{for } c \leq c_1. \end{cases}$$

$$H_{AP}(c) = \begin{cases} 0 & \text{for } c \geq c_2 \\ \bar{\alpha}_1(c_2-c) & \text{for } c_1 \leq c < c_2 \\ \bar{\delta_1}(c_1-c)^n + \bar{\alpha}_1(c_2-c_1) & \text{for } c < c_1 \end{cases} \tag{4}$$

In (4) the constants $\bar{\alpha}_1$ and $\bar{\alpha}_2$ represent the ratio between the height of the activation barrier and the noise intensity, while c_1 and c_2 are defined in Fig. 1. The rationale for these choices is as follows. For concreteness, consider $H_{PA}(c)$. From the discussion in Appendix A, we know that, in the bistable regime (i.e. $c_1 < c \leq c_2$), $H_{PA}(c)$ must be proportional to the ratio between the effective energy barrier and the intensity of the noise. This ratio is given by the parameter $\bar{\alpha}_2$. Moreover, we know that $P_{PA}(c)$, the probability of switching from a proliferating to a quiescent phenotype, must be such that $P_{PA}(c) \to 0$ when $c \geq c_2$ and $P_{PA}(c) \to 1$ when $c \leq c_1$. The former condition implies that $H_{PA}(c)$ must increase rapidly when $c \geq c_2$, and so we assume algebraic dependence on $(c - c_2)$, with exponent $n \gg 1$. The latter condition means that $H_{PA}(c) \to 0$ when $c \to c_1$ and grows as c approaches c_2. The linear dependence on $c - c_1$ in Eq. (4) is the simplest functional form that satisfies these conditions. A similar argument justifies the functional form used for $H_{AP}(c)$ (see Appendix A for a more detailed discussion). The transition probabilities associated with Eq. (4) are plotted in Fig. A1, Supplementary Material, for two different sets of values of $\bar{\alpha}_1$ and $\bar{\alpha}_2$: low noise intensity (green lines in Fig. A1, Supplementary Material) and high noise intensity (red lines in Fig. A1, Supplementary Material).

In the context of the definitions of $\bar{\alpha}_1$ and $\bar{\alpha}_2$, fluctuations are assumed to be produced by intrinsic noise in the intracellular regulatory pathway which generates the bistable response. Intrinsic noise is attributed to finite size effects associated with the regulatory reactions within the cell. Therefore, according to the theory of large deviations (see Appendix A and [33]) $\bar{\alpha}_i \propto V$, where V is the characteristic scale associated with the volume of the cell.

We allow for the general situation in which random transitions between states in the bistable regime are asymmetric, i.e. systems for which transitions in one direction are more likely than in the other. In our model, Eq. (4), this is accounted for by assuming $\bar{\alpha}_1 \neq \bar{\alpha}_2$. If this condition is satisfied, transitions will occur more frequently out of the state with smaller barrier-to-noise ratio. An example of such an asymmetric bistable system has been reported in Hsu et al. (2012), where the evolution of the GAL network in yeast was studied. In this system no transitions were observed from the active to the inactive state, in contrast to inactive-to-active transitions.

3.1 Non-dimensionalisation

We first define the dimensionless time and space variables as $\tau = \tau_p^{-1} t$ and $x \to h^{-1} x$, respectively, where τ_p is the characteristic time for a cell of either type to proliferate or die and h corresponds to the average cell diameter. We further define $\tau_D = h^2/D$ as the characteristic time for oxygen diffusion. With this choice of dimensionless scales, the definition of the dimensionless parameter grouping shown in Table 2 follows naturally.

The values of the parameters used in this paper are given in Table 3.

For simplicity, we further assume that $\alpha_1 = \alpha_2$, $c_1 = 1/2$ and $c_2 = 3/2$. Additionally, we rescale time in the following way: $t \to \epsilon\tau$. In these dimensionless units, the resource equation becomes:

Table 2 Dimensionless variables and parameters

Dimensionless variables	Definition
$c \to c/c_0$	Dimensionless resource concentration
Dimensionless parameter	Definition
$\epsilon = \tau_D/\tau_p$	Ratio between the diffusion time and the proliferation time
$w_0 = \tau_p \bar{w}_0$	Dimensionless characteristic frequency for phenotype switch
$\nu = \tau_p h^{-2} \bar{\nu}$	Dimensionless cellular diffusion coefficient
$\kappa = \tau_D \bar{\kappa}$	Dimensionless resource depletion rate
$\alpha_i = \bar{\alpha}_0 c_i$ $(i = 0, 2, 3)$	See Fig. 1

Table 3 Parameter values used in our simulations

Parameter	Value	Units
ϵ	10^{-4}	Dimensionless
h	10	μm
D	10^3	$\mu\text{m}^2/\text{s}$
$\bar{\kappa}$	10^{-3}	s^{-1}

The values of w_0, α_1, α_2, $\bar{\nu}_2$, and $\bar{\nu}_3$, which are not given in this table, are specified in the captions of specific simulation results. In all simulations we fix $n = 4$, $\bar{\delta}_1 = \bar{\delta}_2 = 1$

$$\frac{\partial c}{\partial \tau} = \nabla^2 c - \kappa c \sum_{k=1}^{N_T} \chi^{(k)} \tag{5}$$

with boundary conditions given by Eq. (2) and initial conditions $c(x, \tau = 0) = 1$.

For a well-mixed system (with no spatial variation), Eq. (5) is superseded by:

$$\frac{dc}{dt} = -\kappa c \sum_{k=1}^{N_T} \chi^{(k)} + S \tag{6}$$

where $S = \kappa \Omega$, so that Eq. (5) admits a spatially-homogeneous, steady-state solution with $c(x) = 1$ and $\sum_{k=1}^{N_T} \chi^{(k)} = \Omega$, i.e. Ω measures the total population that resource levels equivalent to c_0 can sustain. The corresponding dimensionless transition rates are given in Table 4.

4 Well-mixed systems

We start by analysing the well-mixed, spatially-homogeneous version of our model for which the analysis simplifies greatly. Indeed, we find that there exist two asymptotic limits in which it is possible to obtain analytical results.

Table 4 Dimensionless transition rates for our stochastic model of competition between switch-like and bistable populations

Transition rate	Event
$T_{\chi_i^{(1)}+1\|\chi_i^{(1)}} = \epsilon \frac{e^{\alpha_0(c-1)}}{e^{\alpha_0(c-1)}+e^{-\alpha_0(c-1)}} \chi_i^{(1)}$	Division of switch-like cell
$T_{\chi_i^{(1)}-1\|\chi_i^{(1)}} = \epsilon \frac{e^{-\alpha_0(c-1)}}{e^{\alpha_0(c-1)}+e^{-\alpha_0(c-1)}} \chi_i^{(1)}$	Switch-like cell death
$T_{\chi_i^{(2)}+1\|\chi_i^{(2)}} = \epsilon \chi_i^{(2)}$	Proliferation of bistable division
$T_{\chi_i^{(3)}+1\chi_i^{(2)}-1\|\chi_i^{(3)}\chi_i^{(2)}} = \epsilon w_0 e^{-H_{PA}(c)} \chi_i^{(2)}$	Bistable cell phenotype change: proliferating to quiescent
$T_{\chi_i^{(2)}+1,\chi_i^{(3)}-1\|\chi_i^{(2)},\chi_i^{(3)}} = \epsilon w_0 e^{-H_{AP}(c)} \chi_i^{(3)}$	Bistable cell phenotype change: quiescent to proliferating
$T_{\chi_i^{(3)}-1\|\chi_i^{(3)}} = \epsilon \chi_i^{(3)}$	Quiescent cell death
$T_{\chi_i^{(k)}-1,\chi_j^{(k)}+1\|\chi_i^{(k)},\chi_j^{(k)}} = \epsilon \nu_k \chi_i^{(k)}$	Cell migration $\forall k$ and $\forall j \in < i >$

These are obtained by rescaling the transition rates in Table 1

4.1 High barrier-to-noise ratio: Invasion in well-mixed systems

In order to determine whether a mutant bistable population out-competes the resident switch-like population, we adopt a standard two-step procedure Klausmeier (2008), Demetrius et al. (2009): (i) the incumbent population is allowed to evolve in the absence of the invader until it reaches its steady-state population, N_I, and then, (ii) a small number of invasive cells is introduced into the system which continues to evolve until either the invaders out-compete the residents or the invasive species becomes extinct. In the stochastic setting, coexistence is not possible as the system has two absorbing states where either resident or invader becomes extinct. From Eq. (5), it is straightforward to verify that in the absence of invading cells (i.e. $\chi^{(2)} = 0$ and $\chi^{(3)} = 0$) and when spatial effects are neglected (i.e. no diffusion), the steady-state of the incumbent population is given by $N_I = \Omega$ and $c = 1$.

We have conducted numerical simulations in which a population $N_M = yN_I = y\Omega$ of mutants are introduced into a resident population with size $N_I = (1-y)\Omega$, where y is the initial mutant-to-resident ratio and with $c(t=0) = 1$ as the initial resource levels. The system evolve until either the resident population becomes extinct or until a time τ_m has elapsed. In all our simulations we have fixed $\tau_m = 10^6$ which in dimensional terms corresponds to $\tau_m = 100\tau_p$, where τ_p is the cell doubling time. This value of τ_m has been set by running preliminary simulations with different values of τ_m and choosing the smallest value for which statistics were not altered.

We assess which population is the fittest by comparing the probability of invasion, $P_{inv} \equiv P(\chi^{(1)} = 0, \tau \leq \tau_m | \chi^{(2)} + \chi^{(3)} > 0)$, with the results obtained in neutral theory Demetrius et al. (2009). If the mutant were neutral, i.e. it was as fit as the resident, then $P_{inv} = y$ Kimura (1968), Blythe and McKane (2007). Further if $P_{inv} > y$ then the invader is fitter than the resident Demetrius et al. (2009).

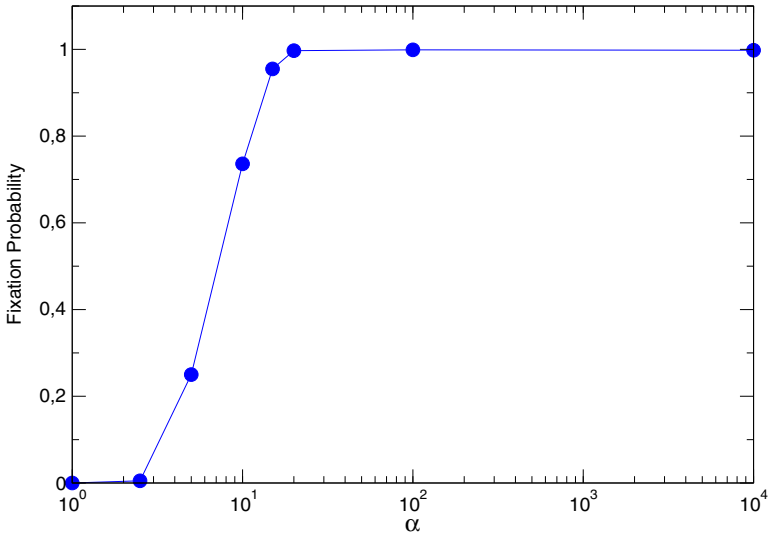

Fig. 2 Simulation results for the fixation probability of the invader (bistable) cell population as a function of the barrier-to-noise ratio $\alpha = \alpha_1 = \alpha_2$. Parameter values: the initial mutant-to-incumbent ratio $y = 1/500$. $w_0 = 10^2$

In Fig. 2 we present simulation results showing how the fixation probability $P_{inv} = P(\chi^{(1)} = 0, \tau \leq \tau_m | \chi^{(2)} + \chi^{(3)} > 0)$ changes as we vary the barrier-to-noise ratio, α. We observe that for low noise intensity the invasion probability is well above that of the neutral case. In fact, for a wide range of values of α, we find that $P(\chi^{(1)} = 0, \tau \leq \tau_m | \chi^{(2)} + \chi^{(3)} > 0) \simeq 1$. For low barrier-to-noise ratio (that is, as the intensity of the intracellular noise increases), the invasion probability decreases until it falls below the neutral case. However, for high barrier-to-noise ratios, i.e. $\alpha_1 = \alpha_2 \gg 1$, the bistable phenotype is fitter than its switch-like counterpart.

4.1.1 Mean-field theory

In order to strengthen our quantitative understanding of the competition between the bistable and switch-like populations, we develop a mean-field theory to describe their interactions. It is straightforward to show that the dimensionless mean-field equations for this process are:

$$\frac{dc}{d\tau} = \kappa\Omega - \kappa\left(n_s + n_p + n_q\right)c, \tag{7}$$

$$\frac{dn_s}{d\tau} = \epsilon \tanh\left(\alpha_0(c-1)\right)n_s, \tag{8}$$

$$\frac{dn_p}{d\tau} = \epsilon n_p - \epsilon w_0 P_{PA}(c) n_p + \epsilon w_0 P_{AP}(c) n_q, \tag{9}$$

$$\frac{dn_q}{d\tau} = -\epsilon n_q + \epsilon w_0 P_{PA}(c) n_p - \epsilon w_0 P_{AP}(c) n_q, \tag{10}$$

where c is the resource concentration, n_s is the number of resident, switch-like cells, n_p and n_q are the number of proliferating and quiescent bistable cells and $\epsilon \ll 1$ is defined in Table 2. The dimensionless parameters in Eqs. (7)–(10) have the same meaning as for their stochastic counterparts. The associated initial conditions are:

$$c(\tau = 0) = 1,\ n_s(\tau = 0) = (1 - y)\Omega,\ n_p(\tau = 0) = n_q(\tau = 0) = y\Omega/2. \quad (11)$$

Note that in the absence of the mutant population, i.e. $n_p = n_q = 0$, the corresponding stable steady-state is given by $c = 1$ and $n_s = \Omega$.

One may ask whether a mean-field theory can accurately predict the behaviour of the stochastic system. To address this question, we have solved numerically Eqs. (7), (9) and (10) with $\Omega = 100$ (see Fig. A2(a), Supplementary Material) and $\Omega = 1000$ (see Fig. A2(b), Supplementary Material) and compared the results to those generated from our stochastic model. The results in Fig. A2, Supplementary Material, show that the mean-field theory provides a reasonable approximation to the full stochastic process, even for system sizes as small as $\Omega = 100$.

Usually, invasion criteria in deterministic systems are based on Malthusian theory where the governing equations are linearised about the relevant attractors and the dominant eigenvalue provides an estimate of the growth rate of the invading population. If the corresponding growth rate is positive then the invading population will eventually displace the resident one. Otherwise, if the growth rate is negative then the incumbent population will resist invasion Metz et al. (1992), Rand et al. (1994), Klausmeier (2008). According to this formulation, the likelihood of invasion by a small mutant population is determined by linearising the dynamics of the invader around the invader-free steady state of the system. In this limit, the equations for the resource levels and the cell populations decouple at $O(\epsilon)$ and we may focus on the linearised equations for n_p and n_q alone. In our case this corresponds to the steady state of Eqs. (7) and (8) with $n_p = n_q = 0$, $c = 1$ and $n_s = \Omega$. The eigenvalue problem corresponding to the linearised system can be written as

$$\frac{dn_p}{d\tau} = \epsilon n_p - \epsilon w_0 e^{-\alpha/2}(n_p - n_q), \quad (12)$$

$$\frac{dn_q}{d\tau} = -\epsilon n_q + \epsilon w_0 e^{-\alpha/2}(n_p - n_q), \quad (13)$$

where, for simplicity, we have assumed that $\alpha = \alpha_1 = \alpha_2$ (i.e. the barriers that bistable cells have to overcome to switch between proliferative and quiescent phenotypes have the same height) determines the ability of the mutant population to invade. Eqs. (12)–(13) have two eigenvalues given by

$$\lambda_\pm = \epsilon\left(-w_0 e^{-\alpha/2} \pm \left(1 + w_0 e^{-\alpha}\right)^{1/2}\right).$$

In Fig. 3 we present results showing how $\lambda = \lambda_\pm/\epsilon$, i.e. the rescaled dominant eigenvalue (the largest positive eigenvalue) associated to the linearised system Eqs. (12)–(13) varies with, α, the barrier-to-noise ratio. We observe an abrupt transition between two regimes: a low noise, large barrier-to-noise ratio (α) regime where $\lambda \simeq 1$

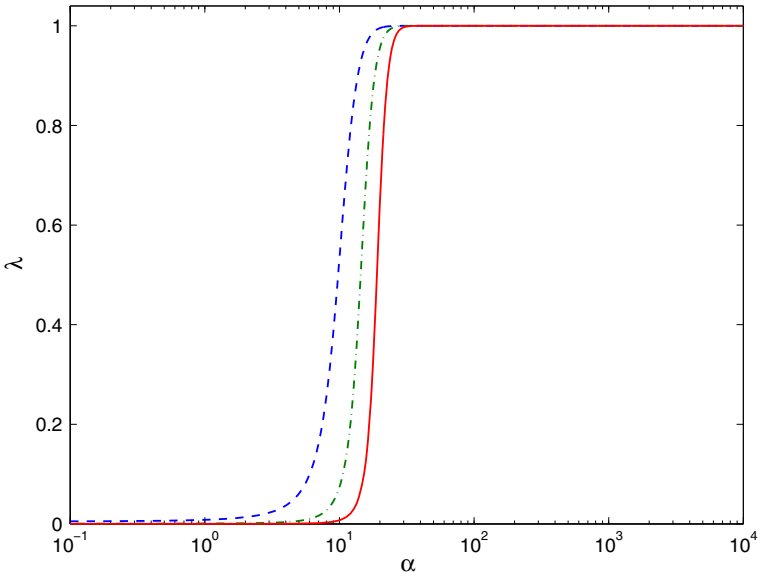

Fig. 3 Series of curves showing how, for different values of w_0, the rescaled dominant eigenvalue, λ, of Eqs. (12)–(13) changes as the barrier-to-noise ration, α, is varied. Key: $w_0 = 10^2$ (*dashed blue line*), $w_0 = 10^3$ (*dash-dotted green line*), and $w_0 = 10^4$ (*solid red line*) (colour figure online)

and a high noise, small barrier-to-noise ratio regime where $\lambda \simeq 0$. The former region corresponds to an invasive mutant which almost certainly takes over the resident population and the latter to a neutral mutant whose invasion likelihood is, according to the neutral theory Kimura (1968), Demetrius et al. (2009), equal to the initial mutant-to-resident ratio (which, in realistic situations, is very small). This analytical result is consistent with simulation results obtained using the SSA Gillespie (1976), Gillespie (1977) and presented in Fig. 2.

Figure 3 also shows how, as w_0 increases (i.e. as the characteristic time for a bistable cell to switch phenotype decreases), the invading regime loses ground to the neutral regime. This is to be expected, as increasing w_0 amplifies the effect of intracellular noise on the bistable population.

In the context of the linear analysis, we have also investigated the behaviour of the bistable population in terms of its ability to invade the switch-like population when the parameters c_1 and c_2 of the bistable cells (see Fig. 1) vary with respect to c_0, the parameter characterising the switch-like cells. More specifically, fixing $c_0 = 1$ for switch-like cells we determined the eigenvalue λ for a range of values of c_1 and c_2. The results are shown in Fig. 4. If $c_1, c_2 < c_0$ (Fig. 4, blue line), we observe that $\lambda > 0$ for all α. This is natural since, according to the scheme in Fig. 1, if $c_1, c_2 < c_0$ then all bistable cells have the proliferative phenotype which gives the invading population an advantage over the resident one. If, on the contrary, $c_0 > c_1, c_2$ (Fig. 4, green line) then $\lambda < 0$ for all α. In this case the invader cells are unable to invade regardless of the value of α. This behaviour can also be understood in terms of Fig. 1: if all bistable cells carry the quiescent phenotype then the resident population has an advantage over the

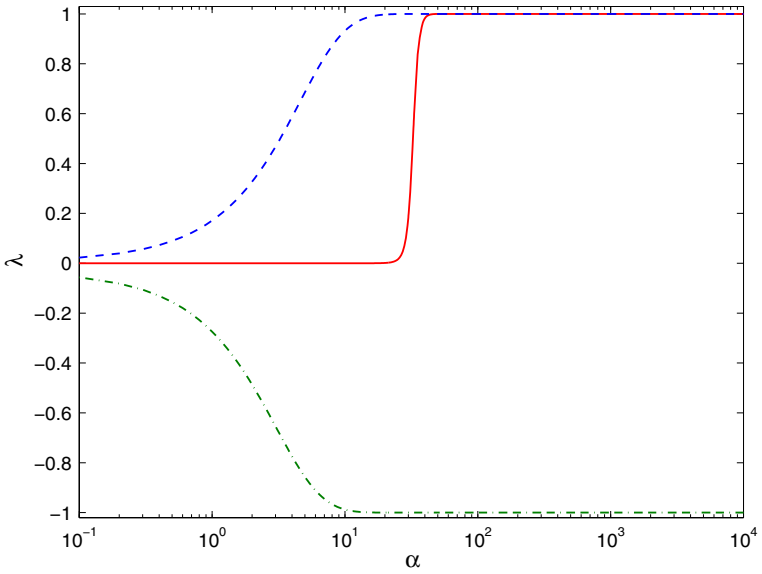

Fig. 4 Series of curves showing how the rescaled dominant eigenvalue, λ, of Eqs. (12)–(13) changes as $\alpha \equiv \alpha_1 = \alpha_2$ varies. We plot λ for different values of c_1 and c_2. Key: $c_1 = 3/2$ and $c_2 = 6/3$ (dash-dotted green line), $c_1 = 2/6$ and $c_2 = 2/3$ (*dashed blue line*), and $c_1 = 1/2$ and $c_2 = 3/2$ (*solid red line*). $w_0 = 10^4$ (colour figure online)

invader one. The third case ($c_1 < c_0 < c_2$) has already been discussed (see discussion regarding Fig. 3).

4.2 Low barrier-to-noise ratio: Dormancy in well-mixed systems

In this section, we analyse our competition model in the low barrier-to-noise ratio limit where $\alpha_1 = \alpha_2 \lesssim 1$. As suggested by the simulation results shown in Fig. 2, as the level of intracellular noise in the bistable population increases, the barrier-to-noise ratio falls and the bistable population loses its competitive advantage with respect to the switch-like population.

4.2.1 Embedded branching process.

In order to understand how this change of behaviour arises, we first look at the numerical simulation of our model and realise that the oxygen concentration remains constant at $c \simeq 1$ (see Fig. A3, Supplementary Material, for a representative realisation of the dynamics of our model in the regime of high intracellular noise). This observation motivates a significant model simplification which enables us to make analytical progress.

If $c \simeq 1$ then the incumbent and mutant populations are effectively decoupled and we can study the (sub)process $(\chi^{(2)}, \chi^{(3)})$ independently of $\chi^{(1)}$ and with constant coefficients (see Table 5).

Table 5 Dimensionless transition rates for our stochastic model for the birth-and-death process of the bistable population

Transition rate	Event
$T_{\chi^{(2)}+1\|\chi^{(2)}} = \epsilon\chi^{(2)}$	Proliferation of bistable cell
$T_{\chi^{(3)}+1\chi^{(2)}-1\|\chi^{(3)}\chi^{(2)}} = \epsilon w_0 e^{-\alpha_2/2}\chi^{(2)}$	Bistable cell phenotype change (proliferating to quiescent)
$T_{\chi^{(2)}+1\chi^{(3)}-1\|\chi^{(2)}\chi^{(3)}} = \epsilon w_0 e^{-\alpha_1/2}\chi^{(3)}$	Bistable cell phenotype change (quiescent to proliferating)
$T_{\chi^{(3)}-1\|\chi^{(3)}} = \epsilon\chi^{(3)}$	Quiescent cell death

These rates are the low barrier-to-noise ratio of the rates given in Table 1. We have also considered the oxygen level to be constant: $c \simeq 1$ (see Fig. A3, Supplementary Materials, for numerical evidence supporting this assumption)

We formulate our analytical theory by considering the embedded branching process equivalent to the birth-death process associated with the transition rates shown in Table 5 Grimmett and Stirzaker (1992). The process of embedding involves coarse-graining time in the following way. After birth, each individual (of type j) lives for a length of time which is exponentially distributed with characteristic time $\tau_c^{(j)} = \left(\epsilon^2(1 + w_0 e^{-\alpha/2})\right)^{-1}$ where $\alpha \equiv \alpha_1 = \alpha_2$. At the end of their life-span, each individual produces offspring according to the corresponding generating functions of the per-cell offspring probabilities Kimmel and Axelrod (2002):

$$G_P(x, y) = \frac{w_0 e^{-\alpha/2}}{1 + w_0 e^{-\alpha/2}} y + \frac{1}{1 + w_0 e^{-\alpha/2}} x^2 \tag{14}$$

$$G_Q(x, y) = \frac{1}{1 + w_0 e^{-\alpha/2}} + \frac{w_0 e^{-\alpha/2}}{1 + w_0 e^{-\alpha/2}} x. \tag{15}$$

For full specification of the age-dependent, embedded branching process, we need to specify the age distribution $f(\tau) = \tau_c^{-1} e^{-\tau/\tau_c}$. By construction, the derivatives of the generating function of the per-cell offspring probability specified in Eqs. (14)–(15) can be used to determine P_{IJ} $(I, J = P, Q)$, the probability that a cell of type J will produce ξ_{IJ} descendants of type I, $P_{IJ} = \frac{1}{\xi_{IJ}!}\partial_I^{\xi_{IJ}} G_J|_{x=y=0}$.

Eqs. (14) and (15) allow us to determine the matrix M, whose entries, $m_{i,j}$, correspond to the average offspring of type i produced by each individual of type j, simply by computing the derivatives of the generating functions:

$$\mathsf{M} = \begin{pmatrix} m_{PP} & m_{PQ} \\ m_{QP} & m_{QQ} \end{pmatrix} = \begin{pmatrix} \partial_x G_P(1,1) & \partial_y G_P(1,1) \\ \partial_x G_Q(1,1) & \partial_y G_Q(1,1) \end{pmatrix} = \begin{pmatrix} \frac{2}{1+\omega} & \frac{\omega}{1+\omega} \\ \frac{\omega}{1+\omega} & 0 \end{pmatrix} \tag{16}$$

where $\omega \equiv w_0 e^{-\alpha/2}$. From elementary considerations in branching process theory Kimmel and Axelrod (2002), we know that, λ_1, the dominant eigenvalue of M, is equal to the growth rate and contains valuable information about the long-term behaviour of our system, including, P_E, the probability of eventual extinction. If $\lambda_1 \leq 1$ then

$P_E = 1$ whereas if $\lambda_1 > 1$ then $P_E < 1$ and the system has a finite probability of long-term survival. With M defined by Eq. (16) we can explicitly calculate λ_1 as:

$$\lambda_1 = \frac{1 + \left(1 + \omega^2\right)^{1/2}}{1 + \omega} \tag{17}$$

which is plotted in Fig. 5 as a function of the parameter $\omega = w_0 e^{-\alpha/2}$. We can see that, as ω increases, our embedded branching process switches from supercritical ($\lambda_1 > 1$) to critical ($\lambda_1 = 1$), i.e. the population transitions from having a positive growth rate to having a zero growth rate. In terms of our competition problem this means that for small ω the bistable population can thrive in the presence of the switch-like population and will therefore eventually invade it. However, as ω increases, the switch-like and the bistable populations engage in a neutral competition scenario, where invasion is a random event whose probability is equal to the initial mutant-to-resident ratio Blythe and McKane (2007), Demetrius et al. (2009). Since, in realistic situations, this ratio is very small, the resulting invasion probability is negligible. This analytic result is in good agreement with the simulation results presented in Fig. 6, where we have plotted the probability of fixation of the invading population $P(\chi^{(1)} = 0, \tau \leq \tau_m | \chi^{(2)} + \chi^{(3)} > 0)$ as a function of w_0. We can see that as w_0 increases, invasion becomes less likely.

4.2.2 *Extinction dynamics of the invading population in the critical case: Emergence of latency in well-mixed systems.*

When studying the competition between two populations it is common practice to look at the growth rate or, correspondingly, the dominant eigenvalue of the growth operator and then to draw conclusions about the invasion probability Klausmeier (2008), Metz et al. (1992), Rand et al. (1994). We would like to extend our argument and analyse the dynamics of the extinction of the invader (bistable) population when they are critical (i.e. when $\omega > 1$). Results from the theory of critical branching processes Holte (1982), Kimmel and Axelrod (2002) show that the long-time asymptotics of the survival probability, $P_S(\tau) \equiv P\left(\chi^{(2)}(\tau) + \chi^{(3)}(\tau) > 0\right)$, exhibits a fat-tail behaviour: $P_S(\tau) \sim A\tau^{-1}$ where the coefficient A is proportional to the inverse of the variance (covariance matrix, for multi-type processes Holte (1982)) of the per-cell offspring probabilities. Accordingly, the probability distribution of the time to extinction, T, has a long-time asymptotic behaviour of the form $f(T) \sim AT^{-2}$. Further, the average extinction time diverges logarithmically, $\mathbb{E}[T] \sim \log(\tau_m)$ as $\tau_m \to \infty$, where τ_m corresponds to the simulation time, and $\mathbb{E}[T^2] \to \infty$. Guided by this asymptotic behaviour we expect that the invading population should be able to survive for arbitrarily long times, with a non-vanishing, albeit small, probability.

The value of the exponent of the survival probability, $P_S(\tau) \sim A\tau^{-\beta}$ with $\beta = 1$, persists for a wide range of critical branching processes Holte (1982). As a result, there is no scope for its control. However, the coefficient A is model-dependent and, therefore, sensitive to changes in the model parameters. Thus, although we cannot change the long-time asymptotics (i.e. the exponent β), we can alter the survival

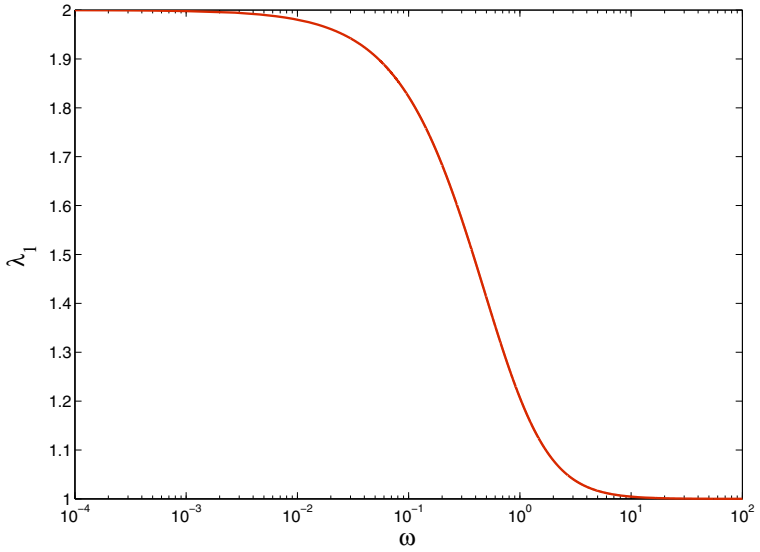

Fig. 5 Dominant eigenvalue, λ_1, of the embedded branching process defined by the generating functions Eqs. (14) and (15) as a function of the parameter $\omega = w_0 e^{-\alpha/2}$ with $\alpha \equiv \alpha_1 = \alpha_2$

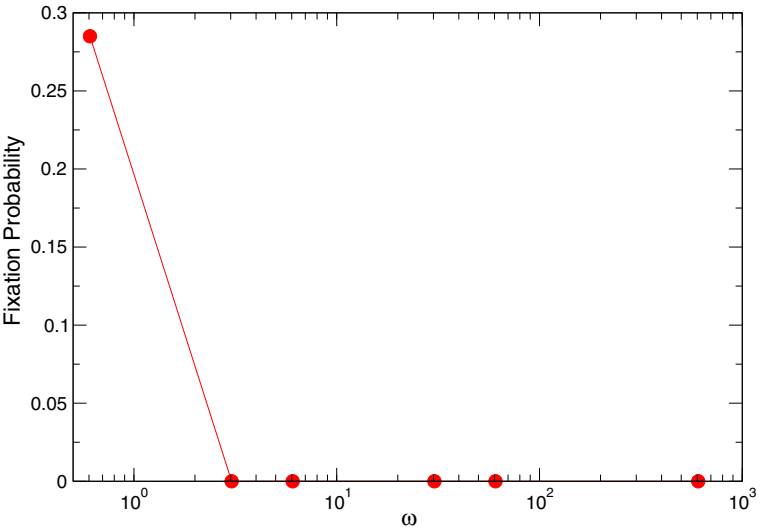

Fig. 6 Invasion probability as a function of ω for $\alpha \equiv \alpha_1 = \alpha_2 = 1$

probability at time τ by varying A. In order to explore this issue further, we need to establish a random benchmark population against which to compare the process defined by Eqs. (14) and (15). We choose as a random benchmark population a single-cell type process for which the probability of proliferation, $P(\xi_R = 2)$, and the probability of death, $P(\xi_R = 0)$, are identical and therefore the growth process is a

Table 6 Dimensionless transition rates for our stochastic model for the birth-and-death process of the random population

Transition rate	Event
$T_{\chi^{(R)}+1\|\chi^{(R)}} = \epsilon\chi^{(R)}$	Random-population cell division
$T_{\chi^{(R)}-1\|\chi^{(R)}} = \epsilon\chi^{(R)}$	Random-population cell death

maximally random, unbiased process. The corresponding generating function, $G_R(x)$, is given by:

$$G_R(x) = \frac{1}{2}(1 + x^2) \tag{18}$$

with $f(\tau) = \tau_c^{-1} e^{-\tau/\tau_c}$ where $\tau_c = \epsilon^{-2}$. The aim of this comparison is to ascertain if bistability has any effect on the long time properties of our system in the critical case ($\omega > 1$). It is trivial to verify that $\mathbb{E}[\xi_R] = 1$ and that $\text{Var}[\xi_R] = 1$. The equivalent birth-and-death process and corresponding Master Equation are determined by the transition rates shown in Table 6.

Notice that the entries of the matrix M specified in Eq. (16) can be written as $\mathsf{M} = (\xi_{IJ} P_{IJ})$ where $I, J = P, Q$, and ξ_{IJ} is a random variable representing the number of offspring of type I produced by a parent of type J, and $P_{IJ} = (1/\xi_{IJ}!)\partial_I^{\xi_{IJ}} G_J|_{x=y=0}$ is the corresponding probability. We can thus define a matrix $\sigma^2 = \left((\xi_{IJ} - \langle\xi_{IJ}\rangle)^2 P_{IJ}\right)$ for $I, J = P, Q$ where:

$$\sigma^2 = \begin{pmatrix} \left(2 - \frac{2}{1+\omega}\right)^2 \frac{1}{1+\omega} & \left(1 - \frac{\omega}{1+\omega}\right)^2 \frac{\omega}{1+\omega} \\ \left(1 - \frac{\omega}{1+\omega}\right)^2 \frac{\omega}{1+\omega} & 0 \end{pmatrix}. \tag{19}$$

and λ_{σ^2}, the dominant eigenvalue of σ^2, is given by:

$$\lambda_{\sigma^2} = \frac{2\omega^2 + w\left(1 + 4\omega^2\right)^{1/2}}{(1+\omega)^3}. \tag{20}$$

In Fig. 7 we use Eq. (20) to show how λ_{σ^2} varies with ω.

Since $\lambda_{\sigma^2} < \text{Var}[\xi_R]$ for $\omega > 0$, for those values of ω for which $\lambda_{\sigma^2} \simeq 1$, we expect that the bistable population, whose population dynamics are determined by the generating functions Eqs. (14) and (15), will exhibit smaller fluctuations and, therefore, be more stable than the random random benchmark population specified in Eq. (18). Further, the coexistence probability at $\tau = \tau_m$ for the bistable population competing against the switch-like population should be bigger than that corresponding to the competition between the random and the switch-like populations. In order to verify these predictions we use the SSA to perform direct simulations.

To check for stability, consider the interval $\mathcal{I} = [0, 100]$. In Fig. 8, we plot R_S, the ratio of the probabilities that the bistable and random populations stay in $\mathcal{I}$ for all $\tau \leq \tau_m$:

$$R_S = \frac{P(\chi^{(1)} > 0, \chi^{(2)} + \chi^{(3)} \in \mathcal{I})}{P(\chi^{(1)} > 0, \chi^{(R)} \in \mathcal{I})}. \tag{21}$$

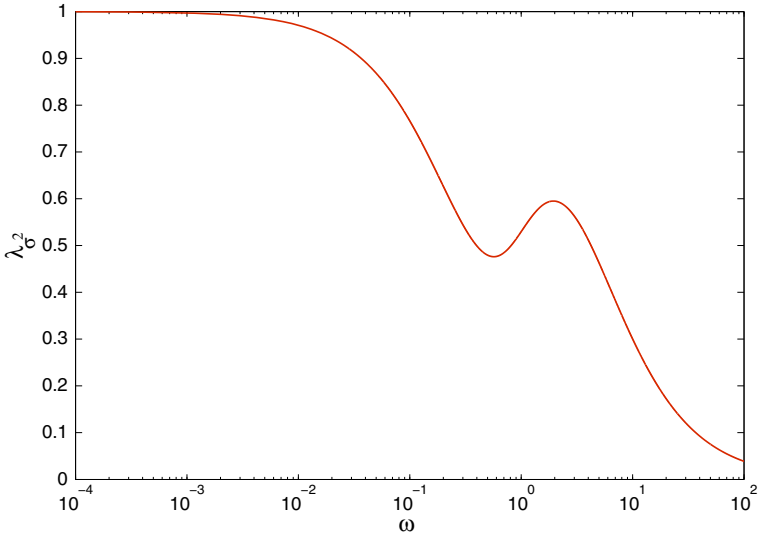

Fig. 7 Dominant eigenvalue, λ_{σ^2}, of the matrix σ^2 Eq. (20) as a function of ω

If the bistable population is more stable than the random benchmark population, we anticipate $R_S > 1$. This is confirmed by the simulation results presented in Fig. 8 where we plot the ratio R_S as a function of ω for $\alpha = \alpha_1 = \alpha_2 = 1$.

To test whether the bistable population is longer-lived than its random counterpart we have computed, for each mutant population, the probability of coexistence between the invader and resident populations after a time τ_m has elapsed, i.e. $P\left(\chi^{(1)}(\tau_m) > 0, \chi^{(2)}(\tau_m) + \chi^{(3)}(\tau_m) > 0\right)$ and $P\left(\chi^{(1)}(\tau_m) > 0, \chi^{(R)}(\tau_m) > 0\right)$, respectively. We define the ratio R_C as:

$$R_C = \frac{P\left(\chi^{(1)}(\tau_m) > 0, \chi^{(2)}(\tau_m) + \chi^{(3)}(\tau_m) > 0\right)}{P\left(\chi^{(1)}(\tau_m) > 0, \chi^{(R)}(\tau_m) > 0\right)}, \tag{22}$$

and deduce that if $R_C > 1$ then the probability of the bistable mutant surviving (without invading the resident population) beyond τ_m is greater than that corresponding to the random mutant. In such cases if the bistable mutant population is unable to invade it is likely to linger for longer times than the random benchmark population. This is to be expected since $\lambda_{\sigma^2} <$Var$[\xi_R]$ and is confirmed by the numerical results presented in Fig. 9.

In Fig. 9 we see that R_C exhibits a non-monotonic dependence on ω, behaviour which is consistent with the non-monotonic behaviour of λ_{σ^2} (see Fig. 7). According to our argument regarding the survival probability of a critical random walk Holte (1982), Kimmel and Axelrod (2002) whereby the smaller the variance the longer-lived the population is expected to be, Fig. 7 shows that as ω increases, λ_{σ^2} exhibits first a minimum, then a maximum, and, after that, a monotonic decrease, which, at the level of the survival probability, should translate into first a maximum, then a minimum,

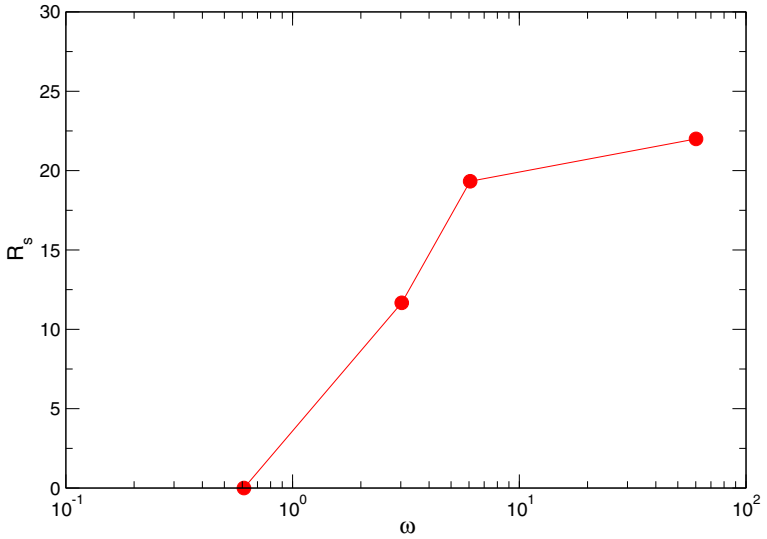

Fig. 8 Ratio R_S, as defined by Eq. (21), as a function of the parameter $\omega = w_0 e^{-\alpha/2}$ with $\alpha = \alpha_1 = \alpha_2 = 1$. The initial mutant population in these simulations, for the competition between the switch-like and random populations, is $\chi^{(R)}(\tau = 0) = 10$, whilst for the competition between the switch-like and bistable populations, it is $\chi^{(2)}(\tau = 0) = \chi^{(3)}(\tau = 0) = 5$

and then a monotonic increase. This scenario is consistent with the behaviour of R_C presented in Fig. 9 and suggests that λ_{σ^2} provides a reasonable description of the variance of the embedded branching process defined by Eqs. (14) and (15).

5 Spatially-inhomogeneous systems

We now study the impact of cell movement and spatial variation on the dynamics of the two cell populations. For simplicity, we focus on the one-dimensional case and the high barrier-to-noise ratio. In particular, we are interested in the effect that cell motility has on the ability of the invading population to invade the resident population.

We start by analysing the low noise regime using a mean-field theory, the natural generalisation of Eqs. (7)–(10) to the spatially-extended case:

$$\frac{\partial c}{\partial \tau} = \frac{\partial^2 c}{\partial x^2} - \kappa(n_s + n_p + n_q)c, \tag{23}$$

$$\frac{\partial n_s}{\partial \tau} = \epsilon \nu_1 \frac{\partial^2 n_s}{\partial x^2} + \epsilon \tanh\left(\alpha_0(c-1)\right) n_s, \tag{24}$$

$$\frac{\partial n_p}{\partial \tau} = \epsilon \nu_2 \frac{\partial^2 n_p}{\partial x^2} + \epsilon n_p - \epsilon w_0 P_{PA}(c) n_p + \epsilon w_0 P_{AP}(c) n_q, \tag{25}$$

$$\frac{\partial n_q}{\partial \tau} = \epsilon \nu_3 \frac{\partial^2 n_q}{\partial x^2} - \epsilon n_q + \epsilon w_0 P_{PA}(c) n_p - \epsilon w_0 P_{AP}(c) n_q, \tag{26}$$

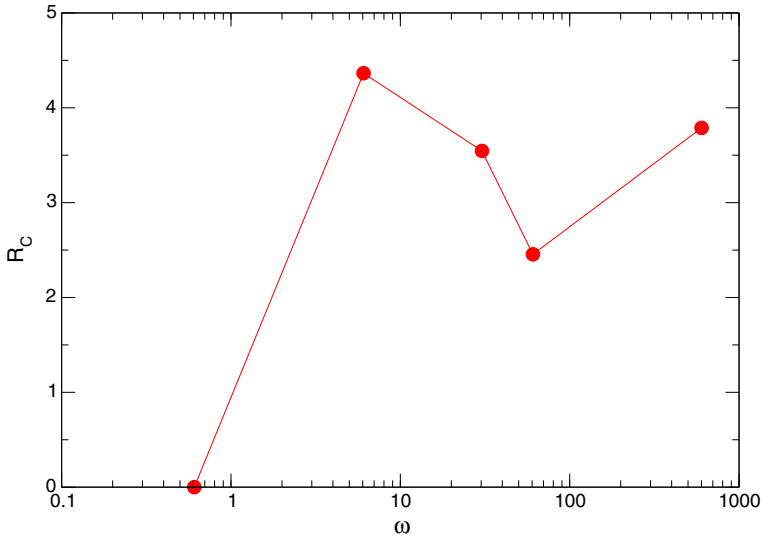

Fig. 9 Ratio R_C, as defined by Eq. (22), as a function of the parameter $\omega = w_0 e^{-\alpha/2}$ with $\alpha = \alpha_1 = \alpha_2 = 1$. The initial mutant population in these simulations, for the competition between the switch-like and random populations, is $\chi^{(R)}(\tau = 0) = 10$, whilst for the competition between the switch-like and bistable populations, it is $\chi^{(2)}(\tau = 0) = \chi^{(3)}(\tau = 0) = 5$

Spatial heterogeneity is induced via flux boundary conditions for the resource concentration,

$$\left.\frac{\partial c}{\partial x}\right|_{x=0} = h_0, \quad \left.\frac{\partial c}{\partial x}\right|_{x=L} = -h_L. \tag{27}$$

whereas no-flux boundary conditions are imposed for the cell populations n_s, n_p and n_q,

$$\left.\frac{\partial n_s}{\partial x}\right|_{x=0} = \left.\frac{\partial n_s}{\partial x}\right|_{x=L} = 0, \quad \left.\frac{\partial n_p}{\partial x}\right|_{x=0} = \left.\frac{\partial n_p}{\partial x}\right|_{x=L} = 0, \quad \left.\frac{\partial n_q}{\partial x}\right|_{x=0} = \left.\frac{\partial n_q}{\partial x}\right|_{x=L} = 0. \tag{28}$$

The initial conditions used to close Eqs. (23)–(26) are:

$$\begin{aligned} &c(x, \tau = 0) = 1 \\ &n_s(x, \tau = 0) = \Omega/L - 2\delta(x - L/2) \\ &n_p(x, \tau = 0) = n_q(x, \tau = 0) = \delta(x - L/2). \end{aligned} \tag{29}$$

where $\delta(x)$ is the Dirac delta distribution i.e., we introduce mutant bistable cells at $x = L/2$. We assume that the resident cells are not motile ($\nu_1 = 0$) whereas the invading population, as part of their evolution towards malignancy, possess a degree of mobility (i.e. $\nu_2 \neq 0$ and $\nu_3 \neq 0$). We solve Eqs. (23)–(26) numerically using the method of lines, performing a finite difference discretisation in space and integrating the resulting ODE system in Matlab via its stiff solver ode23s.

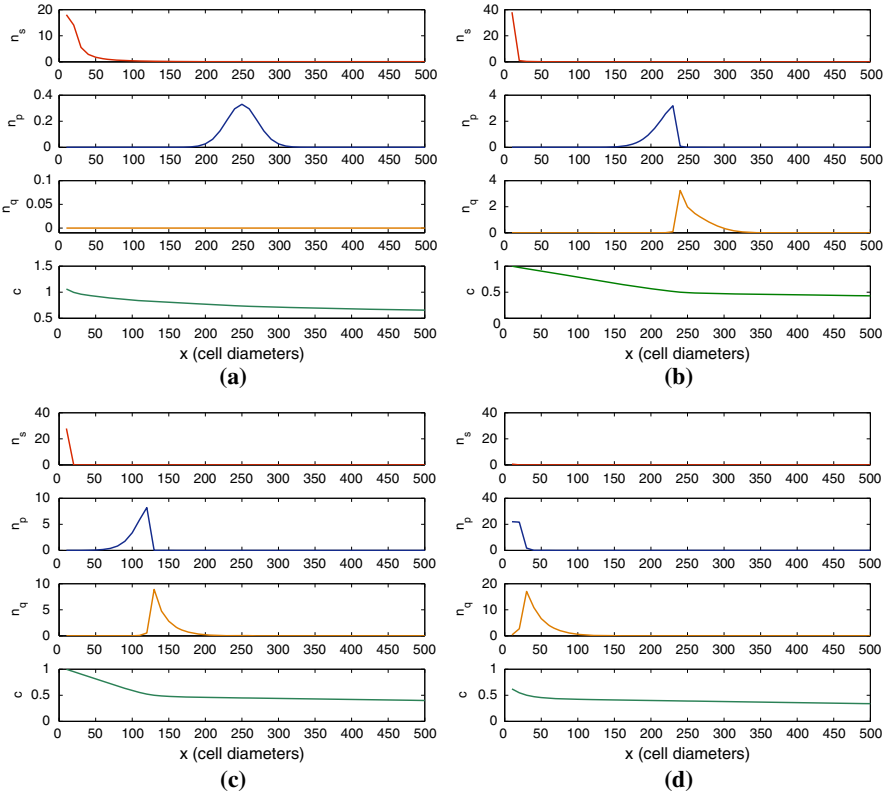

Fig. 10 Four snapshots of the time evolution of Eqs. (23)–(26). Panels (**a**)–(**d**) correspond to $\tau = 2.5 \times 10^4$, $\tau = 5 \times 10^4$, $\tau = 10^5$, and $\tau = 1.5 \times 10^5$, respectively. *Colour code*: *green lines* correspond to $c(x,t)$, *red lines* to $n_s(x,t)$, *blue lines* to $n_p(x,t)$, and *orange lines* to $n_q(x,t)$. Parameter values: $\nu_2 = \nu_3 = 10^{-1}$ $\mu\text{m}^2\text{s}^{-1}$. $w_0 = 10^4$ (colour figure online)

As Fig. 10 reveals, the outcome of the competition between the two populations in a spatial environment is that the bistable population invades the resident one. At early times, the invader cells remain localised in a neighbourhood of the site at which they were seeded. They evolve locally via dynamics similar to those shown in Fig. A2, Supplementary Material. When a sufficiently large number of mutant cells have accumulated, they form an advancing front of proliferative cells which moves up the oxygen gradient. This process continues until the invading population reaches the oxygen-rich region (in our set-up, the region of the domain closer to $x = 0$), where the resident population concentrates. The resident and mutant cells then engage in a competition process similar to that described in Section 4.1, whereupon the resident population becomes extinct.

We now investigate how the outcome of the competition between the switch-like resident and the bistable mutant populations changes as ν_2 and ν_3 vary. We assume that $\nu_2 = \nu_3 > 0$ (all mutant cells are equally motile, regardless of their phenotype) and determine whether the resident population becomes extinct by computing the total population size of each cell type in the domain:

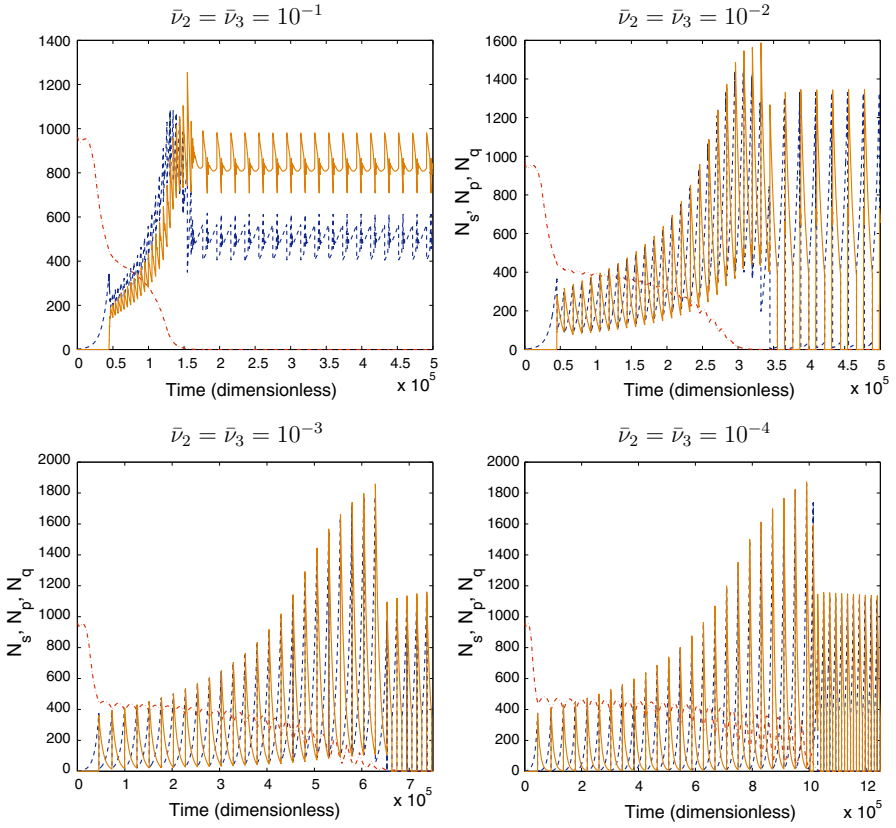

Fig. 11 Series of results obtained from numerical simulations of Eqs. (23)–(29) showing how the time to extinction of the switch-like resident population changes as the motility rate $\bar{n}u_2 = \bar{n}u_3$ of the invading bistable cells varies. Key: $N_s(t)$ (*dash-dotted red lines*), $N_p(t)$ (*dashed blue lines*), $N_q(t)$ (*solid orange lines*) (see Eq. (30)). $\bar{\nu}_1 = 0$. Parameter values: cell diffusion coefficients are given in $\mu\text{m}^2\text{s}^{-1}$, $\bar{\nu}_1 = 0$ and $w_0 = 10^4$ (colour figure online)

$$N_s(t) = \int_0^L n_s(x,t)\,dx,\ N_p(t) = \int_0^L n_p(x,t)\,dx,\ N_q(t) = \int_0^L n_q(x,t)\,dx \quad (30)$$

Typical results are presented in Figs. 11 and 12. Figure 11 shows that the invader cells become more invasive as their motility increases: the four panels in Fig. 11 reveal that the time taken for the invading population to eradicate the resident population increases monotonically as $\nu_2 = \nu_3$ decreases.

Figure 12 shows results for $\nu_2 = \nu_3 = 0$. We see that a non-motile mutant population of mutant cells is unable to invade the resident population in an inhomogeneous environment (generated by an initially heterogeneous distribution of oxygen): the two populations coexist via oscillations, with periods of stasis of the resident population and virtual (although not complete) elimination of the invading population interrupted by bursts of growth and decay.

Taken together, these results suggest that up-regulated cell motility increases the aggressiveness of the bistable mutant, as the time it takes to clear the resident popula-

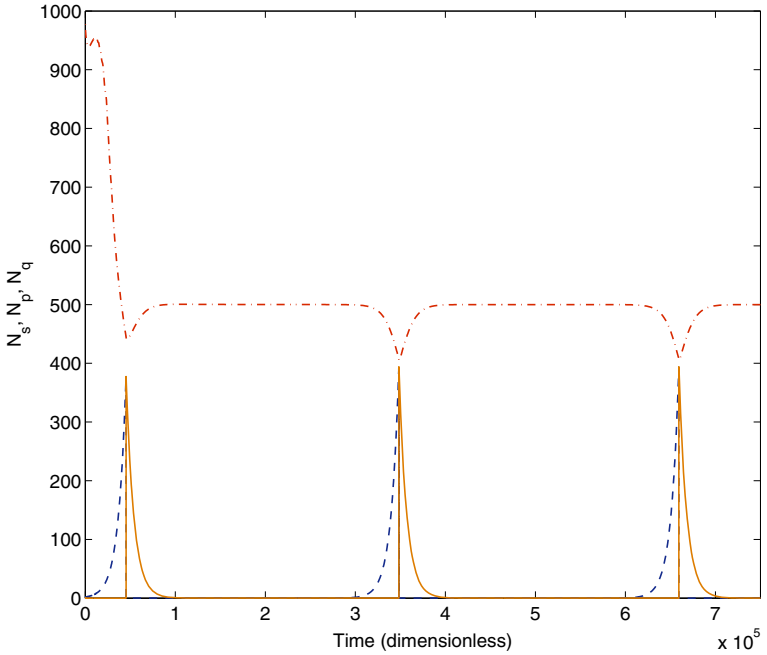

Fig. 12 This plot shows the emergence of coexistence between a motile switch-like resident and a non-motile bistable mutant ($\nu_2 = \nu_3 = 0$). *Dash-dotted red lines* correspond to N_s, *dashed blue lines* to N_p, and *solid orange lines* to N_q. Cell diffusion coefficients are given in $\mu\text{m}^2\text{s}^{-1}$. $w_0 = 10^4$ (colour figure online)

tion is inversely proportional to the cell motility coefficient. Our results also indicate that cell motility may be necessary for invasion into an inhomogeneous environment: if the invader cells are immobile, then both resident and mutant populations coexist in an oscillatory state.

We now proceed to determine whether the increases in invasiveness are induced by cell motility or the bistable structure (i.e. could a mutant cell with switch-like population dynamics and increased motility invade a switch-like, non-motile resident?). We address this question by considering a system in which a non-motile, switch-like population is invaded by a motile, switch-like mutant. In this case, the mean-field dynamics are given by the following system of PDEs:

$$\frac{\partial c}{\partial \tau} = \frac{\partial^2 c}{\partial x^2} - \kappa(n_s + n_m)c \tag{31}$$

$$\frac{\partial n_s}{\partial \tau} = \epsilon \tanh\left(\alpha_0(c-1)\right) n_s \tag{32}$$

$$\frac{\partial n_m}{\partial \tau} = \epsilon \nu_m \frac{\partial^2 n_m}{\partial x^2} + \epsilon \tanh\left(\alpha_0(c-1)\right) n_m, \tag{33}$$

where n_s is the number of (resident) non-motile, switch-like cells and n_m is the number of (mutant) motile, switch-like cells. We prescribe no-flux boundary conditions for

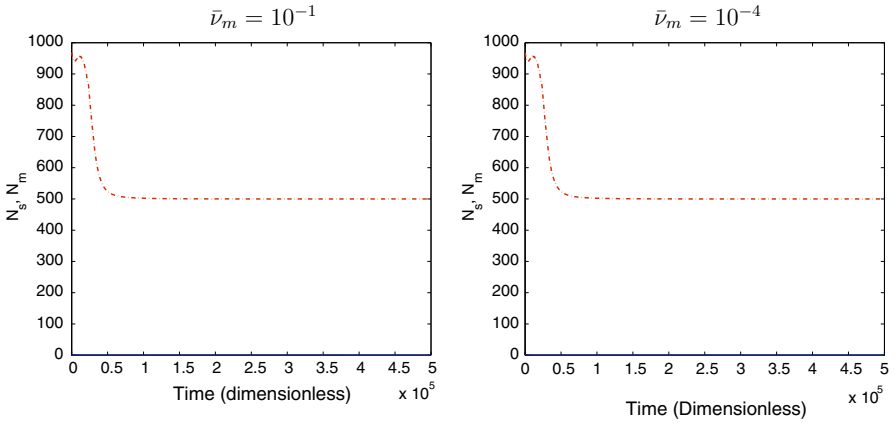

Fig. 13 This plot illustrates that up-regulation of cell motility alone is insufficient to enable a switch-like mutant to invade a resident switch-like population. *Dash-dotted red lines* correspond to N_s and *solid blue lines* to N_m, as defined in Eq. (31). Cell diffusion coefficients are given in $\mu\text{m}^2\text{s}^{-1}$. $w_0 = 10^4$ (colour figure online)

Eq. (33). The boundary conditions for Eq. (31) are given by Eq. (27) with $h_0 - h_L = Lh^{-1}\bar{\kappa}\Omega c_0$. The initial conditions are:

$$\begin{aligned} c(x, \tau = 0) &= 1 \\ n_s(x, \tau = 0) &= \Omega/L - \delta(x - L/2) \\ n_m(x, \tau = 0) &= \delta(x - L/2). \end{aligned} \tag{34}$$

Simulation results showing how the quantities

$$N_s(t) = \int_0^L n_s(x, t)\, dx \text{ and } N_m(t) = \int_0^L n_m(x, t)\, dx \tag{35}$$

evolve over time are presented in Fig. 13 and suggest that increased motility is not sufficient for a mutant population to invade the switch-like population. Rather, that another mutation prior to increased motility (e.g. a mutation leading to bistable cells) is needed in order for the invader cells to invade.

6 Conclusions

In this paper we have presented a model that describes competition between two cell populations for a common (and limited) resource. The populations differ in the strategies that they use to exploit the resource and produce offspring. These alternative strategies are incorporated via response functions, which relate the level of activation of the reproductive pathway (i.e. intracellular levels of cell-cycle-activating proteins) to the amount of resource available (see Fig. 1): whereas the resident population exhibits a sigmoidal, switch-like response curve, the invading population is characterised by

a bistable response curve. We used a variety of mathematical approaches (stochastic simulations, mean-field deterministic differential equations and branching processes theory), to investigate how the ability of the bistable population to invade the switch-like population depends on two factors, the levels of intracellular noise in the bistable cells and their motility. From our analysis, we conclude that:

- For a well-mixed system, the quantity $\omega = w_0 e^{-\alpha/2}$, which measures the effect of noise on the kinetics of phenotype change in bistable cells, plays a key role in controlling the ability of the bistable mutant population to invade the switch-like resident cells: when $\omega \ll 1$, intracellular noise levels are low (see Section 4.1), the bistable population has a competitive advantage and invades the resident switch-like population. If, however, $\omega \gtrsim 1$, and intracellular noise levels are high (see Section 4.1.1), the bistable mutant population loses its competitive advantage and the competition becomes neutral (invasion is a random event, with probability equal to the initial proportion of mutant cells Kimura (1968), Demetrius et al. (2009)). Physically, ω represents the average frequency with which bistable cells change phenotype (from proliferative to quiescent and vice versa). This parameter can be altered by changing either the barrier-to-noise ratio, α, or the characteristic frequency ω_0
- The behaviour of the system in the well-mixed limit when $\omega \geqslant 1$ exhibits a number of features, in particular in its relation to the emergence of latency. In this regime, the dynamics of the bistable mutant population becomes critical in the sense that its net average growth rate is zero and its dynamics become dominated by fluctuations. However, the structure of the bistable population endows it with additional stability, enabling it to be longer-lived than a random population whose individuals do not possess such additional structure. This fact provides a mechanism for latency where small, long-lived mutant colonies do not invade the resident population but persist with non-zero probability until an additional growth-promoting event (e.g. gene mutation) occurs. This scenario could be relevant to a number of long-lived, latent infections, such as HIV-1 under anti-retroviral therapy Rong and Perelson (2009), and also in tumour dormancy Aguirre-Ghiso (2007), Willis et al. (2010), Enderling et al. (2012), Wells et al. (2013).
- Cell motility seems to be a major contributing factor when spatial effects are taken into account. In the low noise limit, we observe that (i) the invader (bistable) cells must be motile if they are to invade, (ii) the aggressiveness of the invading population, measured in terms of the extinction time of the resident population, is positively correlated with the motility of the invader cells, and (iii) a non-motile bistable mutant cannot invade the switch-like resident in spatially inhomogeneous systems. Instead, both resident and mutant populations coexist via a quasi-steady oscillation, with periods of stasis, where the resident population remains constant and the invading population is reduced to very low levels, interrupted by bursts of rapid growth of the bistable mutant, followed by fast decay. Although we have shown that motility increases the likelihood of invasion of our bistable mutant, we have also shown that up-regulation of cell motility alone with no previous transformation is unable to produce an invasive mutant. In our case, this suggests

that a sequence of mutations from switch-like to bistable to motile bistable may produce an aggressive invasive phenotype.

An important issue concerning the applicability of our model to biological situations is noise control at the level of intracellular pathways and gene regulatory networks. Recent studies have concluded that there are a number of mechanisms, including (but not limited to) negative feed-backs and oligomerisation, which act to reduce intracellular noise Becskei and Serrano (2000), Elowitz et al. (2002), Alarcón and Page (2007), Ladbury and Arold (2012). Therefore, in principle, control of the level of intracellular noise is attainable through regulation of such negative feed-backs. Related to control of the levels of intracellular noise, we should also consider whether there are limits on noise suppression Lestas et al. (2010).

We have introduced the hypothesis that all cell types consume oxygen at the same rate. However, it is conceivable that cells using different strategies to utilise resources have different metabolic needs, and, therefore, that we need to consider species-specific oxygen consumption rates Chern et al. (2009). The impact of these factors on the mechanisms that regulate the transition from invasion to latency proposed in this paper is left as an open problem for future work.

Biological applications of our model centre around recent results where positive feed-back loops have been identified as necessary for bistable activation responses in pathways regulating apoptosis Legewie et al. (2006), cell survival Legewie et al. (2007), and cell-cycle progression Ferrel and Xiong (2001). Therefore, one can consider mixed populations in which the different cell types are characterised according to whether these positive feed-backs are functional: cells for which positive feed-back loops are active can be viewed as bistable while cells for which positive feed-backs are inactive, resemble switch-like ones. Such mixed populations, under environmental conditions of limited resources/signalling cues, undergo competition. Our model enables us to investigate which of these response mechanisms is robust in a given environment in terms of the outcome of such competition.

Acknowledgments PG and TA gratefully acknowledge the Spanish Ministry for Science and Innovation (MICINN) for funding under grants MTM2008-05271, MTM2010-18318-E, MTM2011-29342 and Generalitat de Catalunya for funding under grant 2009SGR345. PG thanks the Wellcome Trust for support under grant 098325. This publication was based on work supported in part by Award No. KUK-013-04, made the King Abdullah University of Science and Technology (KAUST).

7 Appendix: Noise in bistable systems

This appendix is devoted to a short summary of the effect of noise in bistable systems. Our aim is not to give a full account of stochastic dynamics of bistable systems, but to provide a brief justification of why phenotype switching in the bistable population can be modelled as an activated process and, consequently, the corresponding transition rates as functions of the Arrhenius type. For a full account, we refer the reader to the the extensive literature on the subject, in particular Gardiner (1983), Maier and Stein (1996), Horsthemke and Lefever (2006), Gardiner (2009).

For concreteness, we consider the following dynamical system:

$$\frac{dx}{dt} = \frac{k_3'(1-x)}{J_3+(1-x)} - \frac{k_4 m y x}{J_4+x}$$
$$\frac{dy}{dt} = k_1 - (k_2' + k_2'' x) y. \tag{36}$$

This system was proposed by Tyson and Novak (2001) as the central component of a more complex pathway regulating the G_1/S transition in the cell-cycle of eukaryote cells. In their original model, x stands for the (normalised) concentration of active Cdh1/APC complexes, y for the concentration of active CycB/CDK complexes, and m for the cell size. Here, m will be assumed to be the control parameter.

As m increases, Eqs. (36) go through a series of bifurcations which separate different regimes (see Fig. 14): For small values of m the system exhibits a single steady-state (high x = Cdh1, low y = CycB corresponding to G_1). Intermediate values of m lead to a bistable regime where two stable steady-states (high Cdh1, low CycB corresponding to G_1 and low Cdh1 and high CycB, corresponding to S–G_2–M) coexist with a saddle point. Finally, as m continues to increase a saddle-node bifurcation occurs which leads to the annihilation of the G_1-like steady-state and the saddle point. In each of the panels of Fig. 14, we show two solutions of Eqs. (36) corresponding to two different initial conditions: $y(t=0) = 0.28$ and $x(t=0) = 0.9$ (solid green lines) and $y(t=0) = 0.3$ and $x(t=0) = 0.9$ (solid purple lines). We have also plotted realisations of a stochastic system equivalent to Eqs. (36) (see Guerrero and Alarcón (2015) for details) with the same initial conditions (dashed green lines and dashed purple lines, respectively). In the two mono-stable cases shown in panels $m = 0.01$ and $m = 1$, we see that there are no major differences in behaviour between the mean-field (solid lines) and the stochastic (dashed lines) systems: In both cases the stochastic trajectories converge toward the mean-field fixed point, regardless of the initial condition. The behaviour in the bistable regime offers more possibilities. We have chosen the initial conditions (for both the mean-field equations and the stochastic system) so that they belong to different basins of attraction of the mean-field system: $y(t=0) = 0.28$ and $x(t=0) = 0.9$ (solid green lines) belongs to that of G_1, $y(t=0) = 0.3$ and $x(t=0) = 0.9$ (solid purple lines), to that of S-G_2-M the bistable regime ($m = 0.2$). In this regime, we can see that the stochastic trajectories (dashed lines) may either behave like their mean-field counterparts and converge towards the corresponding steady-state, or, on the contrary, jump across the separatrix and converge towards the steady-state corresponding to the other (mean-field) basin of attraction.

Let us focus now on the bistable regime (e.g. $m = 0.2$ in Fig. 14). If noise is ignored, then the stable steady-states have disjoint basins of attraction, being separated by a separatrix which passes through the saddle: If the initial condition is contained in the G_1-basin (respectively, S-G_2-M) then the system will evolve towards G_1 (respectively, S-G_2-M). By contrast, if noise is taken into account then the separatrix becomes a barrier that the system may cross with finite probability. This is shown in Fig. 14 where we compare the solution of Eqs. (36) with two different initial conditions, one on each side of the separatrix, with a stochastic version of the Tyson & Novak model developed in Guerrero and Alarcón (2015).

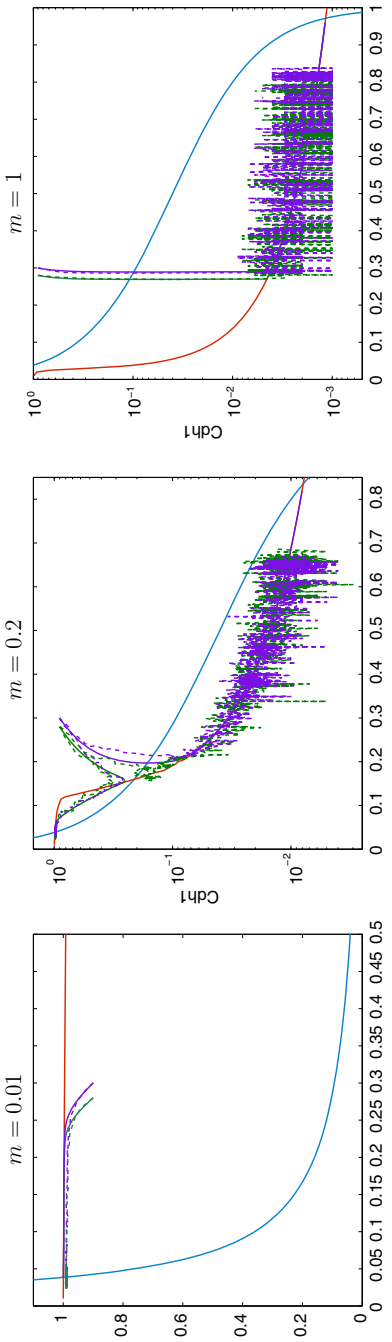

Fig. 14 Phase spaces showing the three possible steady-state regimes associated with Eqs. (36) for different values of the control parameter m. In all *three panels* the *solid blue line* corresponds to the y-nullcline and the red line to the x-nullcline. The intersections between both nullclines correspond to the fixed points of Eqs. (36). For small values of m, e.g. $m = 0.01$, the only (stable) fixed point is the G_1-like steady-state. For intermediate values of m, e.g. $m = 0.2$, Eqs. (36) exhibit bistability: The system has two stable steady states (G_1 and S-G_2 – M) and an unstable fixed (saddle) point. For large values of m, e.g. $m = 1$, the only (stable) fixed point is the S-G_2-M-like steady-state. Parameter values: $k_1 = 0.04\,\mathrm{min}^{-1}$, min^{-1}, $k_2' = 0.04\,\mathrm{min}^{-1}$, $k_2'' = 1$, $k_3' = 1\,\mathrm{min}^{-1}$, $k_4 = 35\,\mathrm{min}^{-1}$, $J_3 = J_4 = 0.04$ Tyson and Novak (2001) (colour figure online)

There is extensive literature Escudero and Kamenev (2009), Gardiner (1983), Gardiner (2009), Horsthemke and Lefever (2006), Maier and Stein (1996) showing that, in the limit of low noise intensity, σ, the process of switching between two stable states is an activated process, i.e. the transition rate from one steady state to the other, W_T, is such that $W_T \sim e^{-H}$ for $\sigma \ll 1$ where H is a function of the parameters of the system.

While a detailed mathematical derivation is beyond the scope of this appendix, the physical rationale is relatively straightforward Kubo et al. (1973). In equilibrium statistical mechanics, the statistical distribution for an extensive variable, say X, is given by $P_e(X) = Z^{-1} e^{-\frac{V}{k_B T}\phi_e(x)}$, where V is the volume of the system, $x = X/V$, $k_B T$ is the energy associated with thermal noise (T is the temperature and k_B is Boltzmann's constant), and $\phi_e(x)$ is the equilibrium free energy per unit volume. From elementary considerations in equilibrium thermodynamics, we know that the equilibrium value of x corresponds to the minimum of $\phi_e(x)$ which, in turn, corresponds to the most probable value of x according to the probability distribution $P_e(X)$, with $P_e(X)$ providing the probability of deviation of x from its *optimal* value, x_e. Incidentally, we remark that for low noise intensity, i.e. for $k_B T$ much smaller than a characteristic energy scale associated with $\phi_e(x)$, large deviations from x_e are very unlikely as they are exponentially suppressed Touchette (2009). We note also that the larger the size of the system, V, the more insensitive the system becomes to random effects.

The essential ansatz leading to $W_T \sim e^{-H}$ is that non-equilibrium (i.e. time-evolving) states of *large* systems can be described by a probability distribution which is a straightforward generalisation of P_e, i.e.:

$$P(X(t)|X_0) = \mathcal{C} e^{-\frac{V}{\sigma}\phi(x(t)|x_0)} \tag{37}$$

where $x(t) = X(t)/V$ is a sample path or realisation of the stochastic process, $x_0 = x(0)$ denotes the initial condition and σ is the intensity of the noise (which plays the same role as the temperature $k_B T$ in the equilibrium case). Therefore, the most likely evolution for $x(t)$ is along the path that minimises $\phi(x(t)|x_0)$, and $P(X(t)|X_0)$ can, again, be understood as the probability that a sample path deviates from the optimal (most probable) path, $x_o(t)$. For large systems, $\Omega \gg 1$, such deviations are very unlikely (they are exponentially suppressed) and the most significant contribution comes from $x_o(t)$. Hence, provided the noise $\sigma \equiv V^{-1} \ll 1$, the transition probability of the system to start from X_0 and evolve to a state X_1 at time t, W_T, can be estimated by taking $\phi = \phi_0 \equiv \phi(x_o(t)|x_0)$ in Eq. (37), namely, $W_T \sim e^{-H}$ where $H \equiv \frac{V}{\sigma}\phi_0$.

Although we have presented this argument in an heuristic (non-rigorous) way, it can be made mathematically rigorous within the framework of the theory of large deviations Kubo et al. (1973), Touchette (2009).

References

Aguirre-Ghiso JA (2007) Models, mechanisms and clinical evidence for cancer dormancy. Nat Rev Cancer 7:834–846

Alarcón T, Byrne HM, Maini PK (2004) A mathematical model of the effect of hypoxia on the cell-cycle of normal and cancer cells. J Theor Biol 229:395–411
Alarcón T, Page KM (2006) Stochastic models of receptor oligomerisation by bivalent ligand. J R Soc Interface 3:545–559
Alarcón T, Page KM (2007) Mathematical models of the VEGF receptor and its role in cancer therapy. J R Soc Interface 4:283–304
Alarcón T, Jensen HJ (2010) Quiescence: a mechanism for escaping the effects of drug on cell populations. J R Soc Interface 8:99–106
Becskei A, Serrano L (2000) Engineering stability in gene networks by autoregulation. Nature 405:590–593
Bedessem B, Stéphanou A (2014) A mathematical model of HIF-1-α-mediated response to hypoxia on the G1/S transition. Math Biosci 248:31–39
Blythe RA, McKane AJ (2007) Stochastic of evolution in genetics, ecology and linguistics. J Stat Mech P07018. doi:10.1088/1742-5468/2007/07/P07018
Bruna M, Chapman SJ (2012) Excluded-volume effects in the diffusion of hard spheres. Phys Rev E 85:011103
Chern Y, Cairns R, Papandreou I, Koong A, Denko NC (2009) Oxygen consumption can regulate the growth of tumours. A new perspective on the Warburg effect. PLoS One 4:e7033
Demetrius L, Gundlach VM, Ochs G (2009) Invasion exponents in biological networks. Physica A 388:651–672
Elowitz MB, Levine AJ, Siggia ED, Swain PS (2002) Stochastic gene expression in a single cell. Science 297:1183–1186
Enderling H, Almog N, Hlatky L (eds) (2012) Systems biology of tumour dormancy. Springer-Verlag, New York
Escudero C, Kamenev A (2009) Switching rates in multistep reactions. Phys Rev E 79:041149
Ferrel JE, Xiong W (2001) Bistability in cell signalling: how to make continuous processes discontinuous, and reversible processes irreversible. Chaos 11:227–236
Gardiner CW (1983) The escape time in nonpotential systems. J Stat Phys 30:157–177
Gardiner CW (2009) Stochastic methods. Springer-Verlag, Berlin
Gillespie DT (1976) A general method for numerically simulating the stochastic time evolution of coupled chemical reactions. J Comput Phys 22:403–434
Gillespie DT (1977) Exact stochastic simulation of coupled chemical reactions. J Phys Chem 81:2340–2361
Golbeter A, Koshland DE (1984) Ultrasensitivity in biochemical systems controlled by covalent modification. Interplay between zero-order and multistep effects. J Biol Chem 259:14441–14447
Guerrero P, Alarcón T (2015) Stochastic multiscale models of cell populations: asymptotic and numerical methods. Math Model Nat Phen 10:64–93
Grimmett GR, Stirzaker DR (1992) Probability and random processes. Oxford University Press, Oxford
Hanggi P, Talkner P, Borkovec M (1990) Reaction rate theory: 50 years after Kramers. Rev Mod Phys 62:251–341
Holte JM (1982) Critical multi-type branching processes. Ann Probab 10:482–495
Horsthemke W, Lefever R (2006) Noise-induced transitions. Springer-Verlag, New York
Hsu C, Scherrer S, Buetti-Dinh A, Ratna P, Pizzolato J, Jaquet V, Becskei A (2012) Stochastic signalling rewires the interaction map of multiple feedback network during yeast evolution. Nat Commun 3:682
Kelemen J, Ratna P, Scherrer S, Becskei A (2010) Spatial epigenetic control of mono- and bistable gene expression. PLoS Biol 8:e1000332
Kholodenko BN (2000) Negative feedback and ultrasensitivity can bring about oscillations in the mitogen-activated protein kinase cascades. Eur J Biochem 267:1583–1588
Kimura M (1968) Evolutionary rate at the molecular level. Nature 217:624–626
Kimmel M, Axelrod DE (2002) Branching processes in biology. Springer-Verlag, New York
Klausmeier CA (2008) Floquet theory: a useful tool for understanding non-equilibrium dynamics. Theor Ecol 1:153–161
Kitano H (2004) Cancer as a robust system: implications for cancer therapy. Nat Rev Cancer 4:227–235
Kubo R, Matsuo K, Kitahara K (1973) Fluctuation and relaxation of macrovariables. J Stat Phys 9:51–96
Ladbury JE, Arold ST (2012) Noise in cellular signalling pathways: causes and effects. Trends Biochem Sci 37:173–178
Legewie S, Blüthgen N, Herzel H (2006) Mathematical modelling identifies inhibitors of apoptosis as mediators of positive feed-back and bistability. PLoS Comput Biol 2:e120

Legewie S, Blüthgen N, Herzel H (2007) Competing docking interactions can bring about bistability in the MAPK cascade. Biophys J 93:2279–2288
Lestas I, Vinnicombe G, Paulsson J (2010) Fundamental limits on the suppression of molecular fluctuations. Nature 467:174–178
Lugo C, McKane AJ (2008) Quasicycles in a spatial predator–prey model. Phys Rev E 78:051911
Maier RS, Stein DL (1996) A scaling theory of bifurcations in the symmetric weak-noise escape problem. J Stat Phys 83:291–357
Metz JAJ, Nisbet RM, Geritz SAH (1992) How should we define "fitness" for general ecological scenarios? Trends Ecol Evol 7:198–202
Munoz MA, Grinstein G, Tu Y (1997) Survival probability and field theory in systems with absorving states. Phys Rev E 56:5101–5105
Ortega F, Garcés JL, Mas F, Kholodenko BN, Cascante M (2006) Bistability from double phosphorylation in signal transduction. Kinetic and structural requirements. FEBS J 273:3915–3926
Rand DA, Wilson HB, McGlade JM (1994) Dynamics and evolution: evolutionarily stable attractors, invasion exponents and phenotype dynamics. Philos Trans R Soc Lond B 343:261–283
Rong L, Perelson AS (2009) Modelling latently infected cell activation: viral and latent reservoir persistence, and viral blips in HIV-infected patients on potent therapy. PLoS Comput Biol 5:e1000533
Strogatz SH (1994) Nonlinear dynamics and chaos. Perseus Books, New York
Tian T, Olson S, Whitacre JM, Harding A (2011) The origin of cancer robustness and evolvability. Integr Biol 3:17–30
Touchette H (2009) The large deviation approach to statistical mechanics. Phys Rep 479:1–69
Tyson JJ, Novak B (2001) Regulation of the eukaryotic cell cycle: molecular antagonism, hysteresis, and irreversible trasitions. J Theor Biol 210:249–263
Tyson JJ, Chen KC, Novak B (2003) Sniffers, buzzers, toggles and blinkers: dynamics of regulatory and signalling pathways in the cell. Curr Opin Cell Biol 15:221–231
Wells A, Griffith L, Wells JZ, Taylor DP (2013) The dormancy dilemma: quiescence versus balanced proliferation. Cancer Res 73:3811–3816
Willis L, Alarcón T, Elia G, Jones JL, Wright N, Graham TA, Tomlinson IPM, Page KM (2010) Breast cancer dormancy can be maintained by a small number of micrometastases. Cancer Res 70:4310–4317